Robotics and Autonomous Systems 62 (2014) 1016–1033

Contents lists available at ScienceDirect

Robotics and Autonomous Systems

journal homepage: www.elsevier.com/locate/robot

Roombots: A hardware perspective on 3D self-reconfiguration and locomotion with a homogeneous modular robot

A. Spröwitz *, R. Moeckel, M. Vespignani, S. Bonardi, A.J. Ijspeert

Biorobotics laboratory, École polytechnique fédérale de Lausanne, EPFL STI IBI BIOROB Station 14, 1015 Lausanne, Switzerland

HIGHLIGHTS

- We designed, implemented, and tested the Roombots (RB) modular robots.
- We explain the RB design methodology: active connection mechanism and module.
- RB use locomotion on-grid (lattice-based environment), and off-grid locomotion.
- RB join into metamodules on-grid, and can transit from off-grid to on-grid.
- We demonstrate RB overcoming concave and convex edges, and climbing vertical walls.

ARTICLE INFO

Article history:
Available online 2 September 2013

Keywords:
Self-reconfiguring
Modular robots
Active connection mechanism
Module joining
Module climbing
Grid environment
Homogeneous modular robotic system

ABSTRACT

In this work we provide hands-on experience on designing and testing a self-reconfiguring modular robotic system, Roombots (RB), to be used among others for adaptive furniture. In the long term, we envision that RB can be used to create sets of furniture, such as stools, chairs and tables that can move in their environment and that change shape and functionality during the day. In this article, we present the first, incremental results towards that long term vision. We demonstrate locomotion and reconfiguration of single and metamodule RB over 3D surfaces, in a structured environment equipped with embedded connection ports. RB assemblies can move around in non-structured environments, by using rotational or wheel-like locomotion. We show a proof of concept for transferring a Roombots metamodule (two in-series coupled RB modules) from the non-structured environment back into the structured grid, by aligning the RB metamodule in an entrapment mechanism. Finally, we analyze the remaining challenges to master the full Roombots scenario, and discuss the impact on future Roombots hardware.

1. Introduction

We are working towards the idea of a living environment where classic roomware components are merged and enhanced by elements from robotics and information technology. We tackle this task by designing Roombots (RB), an instance of self-reconfiguring modular robots (SR-MR) which are meant to be embedded into our living environment, to build intelligent furniture and other components of our daily life. Self-reconfiguring modular robots are highly integrated, self-sustaining robotic building blocks with limited degrees of freedom (DOF). A number of them can connect to each other with active connection mechanisms (ACM), creating a robot or structure with more capabilities than a single module. Eventually, we see the task of RB to build adaptive furniture that connects into different shapes, such as stools, tables, or sofas. It should also adapt to the user's needs, by changing shape over time, and by moving around.

Several designs of self-reconfiguring modular robotic systems have been proposed, with the goal to assemble larger structures [1,2]. Such structures could be complex assemblies, such as parts of a space station, remote, hard-to-reach and hard-to-maintain systems such as a modular satellite, deep-sea underwater structures, or scaffolds. For the Roombots project, we are aiming to assemble furniture-like structures. For our furniture, we want to minimize the number of active robotic modules by combining active modules and passive elements—a table assembled from light-weight elements and a few Roombots modules would be by far cheaper, less heavy and structurally more sound than one made entirely from modular robots. Currently, we envision a mix of Roombots modules and passive elements, as depicted in Fig. 1. Light-weight elements of several shapes and Roombots modules would create a patchwork, held together by Roombots modules. Connector "ports" play an important role in this scenario; these are distributed around the room as passive connectors in the floor, walls, ceilings, and within the light-weight elements. The same ports are also part of Roombots modules, as its active and passive connectors.

Towards this future goal, we tackle and present experimental results for five sub-scenarios in this work. Firstly, we imagine a

* Corresponding author. Tel.: +41 216932644.
E-mail addresses: alexander.sproewitz@epfl.ch, alexspr@gmail.com (A. Spröwitz).

0921-8890/$ – see front matter
http://dx.doi.org/10.1016/j.robot.2013.08.011

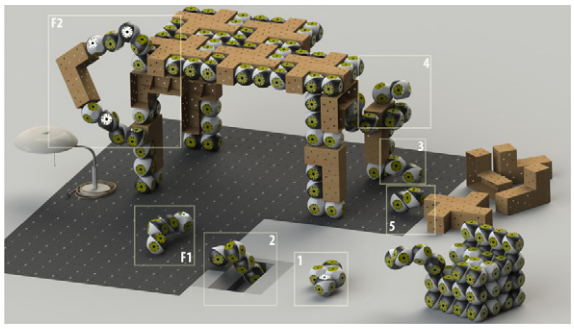

Fig. 1. Rendered vision of a table being assembled by Roombots (RB) modules, from light-weight elements and integrated RB modules. Tiles on the floor are connector ports. Those, and connectors embedded in modules and passive elements enable Roombots to grab onto. In this work, we show proof of concept experiments with two types of RB metamodule locomotion on non-structured ground (subtask 1), RB metamodule alignment into the structured grid though an entrapment mechanism (subtask 2), RB locomotion on a structured grid, approaching and overcoming of a concave corner (subtask 3), and a Roombots module climbing up vertical structures and overcoming convex corners by merging with a Roombots "helper" module (subtask 4). For the future, open-loop, on-grid locomotion of RB metamodules will enhance locomotion and reconfiguration speed (future subtask F1). Further, handling of light-weight, structural objects by two enhanced RB metamodules (future subtask F2) is planned to assemble large structures, such as this table. Currently, Roombots hardware only performs simpler pick-up moves, such as shown with the light-weight plates. Subtask 5 is a simplified task, and demonstrates the concept. The lamp was added for size comparison.

stock of Roombots modules on the side, and modules detaching from it. Not all the floor will be equipped with connector ports. To reach a port-equipped area ("on-grid"), we show how pairwise connected Roombots metamodules (MM) locomote with oscillating or wheel-like rotating motion patterns over the floor ("off-grid" locomotion, Fig. 1, subtask 1). Module locomotion is controlled by a central pattern generator (CPG) [3] implemented as a network of coupled oscillators, distributed in the different modules. CPG are decentralized and well suited to organize rhythmic and non-rhythmic motions of large numbers of modular robots.

Next, modules have to become aligned to the grid. We propose a passive mechanism based on an entrapment-like structure (Fig. 1, subtask 2): Roombots metamodules slide into a sink-like entrapment mechanism (EM). In there the MM automatically aligns, the MM's ACM grippers connect to a EM wall port. With a couple of predefined joint moves the MM leaves the EM, and "brachiates" over the grid connection ports [4,5] (simulation results). Roombots modules can perform on-grid locomotion by iteratively attaching and detaching to the ports. In some cases, modules fail to attach when controlled in open-loop because of excessive bending of the structure, and necessary hardware updates for this task are discussed in Section 5.

To build a larger structure from modules and passive elements, Roombots modules will have to approach, climb, and overcome walls and planes. Those obstacles present themselves either as "concave" edges, planes, or "convex" edges. Single Roombots modules are designed and controlled to overcome concave edges (Fig. 1, subtask 3), and to switch from a horizontal plane to a vertical plane. To go upwards and switch to the next-level horizontal plane a single Roombots module has to be merged into a full Roombots metamodule, together with a Roombots "helper module" (Fig. 1, subtask 4).

Roombots are meant to assemble larger structures from passive elements. In subtask 5 we present a brief first step towards handling light-weight structures. In fact, the future Roombots hardware will require a stiffness and power upgrade before being able to handle larger elements, as depicted on the left side of the figure. For now, two Roombots modules are picking up a pair of light-weight connector plates (Fig. 1, similar to 5). For the future of this project, remaining challenges will include the tasks of picking up light-weight elements by cooperating Roombots metamodules, transporting those elements to their assembly point (Fig. 1, two metamodules lifting a light-weight element to the table top), and finally mounting and assembling everything into meaningful structures. In this work we focus at the defined five subtasks and the necessary modular robot hardware to robustly solve these scenarios. Remaining challenges (e.g. multi-metamodule handling of passive elements, RB metamodule locomotion on-grid) are identified along with this work, and are analyzed and discussed in Section 5.

The paper is structured as follows: Section 2 gives a brief overview over modular robot (MR) classifications, and significant MR implementations. In Section 3 we present the mechanical, electrical, and control design of Roombots. In Section 4, we show five hardware experiments of reconfiguration and locomotion on-grid and off-grid, in 2D and in 3D, alignment of RB from off-grid to on-grid, and handling of light-weight elements through RB modules. We discuss our results and future work in Section 5, and conclude the paper in Section 6.

2. Related work

In this section, we survey and analyze a selection of modular robots, with a focus on module density, weight, and classification of modular robots. The background of this survey is the Roombots scenario, and the core tasks of RB modules (a) to attach and detach robustly with other RB modules and the environment, (b) to locomote with brachiating movements through the surrounding on-grid environment and move in the off-grid environment and (c) to handle other RB modules and light-weight elements. We aim to identify successful blueprints in existing MR projects that can contribute to solving the RB scenario or guide the mechanical design process of such a self-reconfiguring modular robot.

MR research aims to increase robustness by replacing faulty parts of a robot structure by a functioning module. Active connection mechanisms (ACM) are the characteristic component of self-reconfiguring modular robots (SR-MR) which can actively, and autonomously, attach and detach modules to and from a structure. Units can rapidly be replaced, because every module has a high degree of autonomy. Modular robotic systems, or "cellular robots" [6], are often designed as self-sufficient systems. Every module will include actuation, computation, sensing, power supply, connection mechanisms, and a shell structure. If all modules are designed identical, a modular robot system is homogeneous [7]. Because such high integration is expensive in terms of complexity, maintenance, redundancy, weight, and time to design, several MR systems are designed as heterogeneous systems [8], with a subset of functionally different cells, but common connectors, interfaces, and grid size. *Stochastic modular robots* are modules that float, glide or swim in 2D or 3D [9–11]. They draw energy from their environment. Further, stochastic modular robots have the potential for massive parallel, rapid self-assembly. This is a similar approach to nano-scale structures made from DNA molecules [12]. Many freely moving, non-connected modules present a significant organization and control challenge, in terms of communication, computation, timing, and absolute and relative position sensing of neighboring modules. *Grid based* modules are either connected to an outside grid structure, or neighboring modules. They can use this mechanical connection to communicate and self-orient. Many MR are implemented as *lattice grid* based MR (e.g. the ATRON robot [13]), with a lattice similar to that of a crystal. Certain module designs result in *tree or chain-like structures*. Such MR are often used as building blocks for robots moving *off-grid*, in the unstructured environment with no available

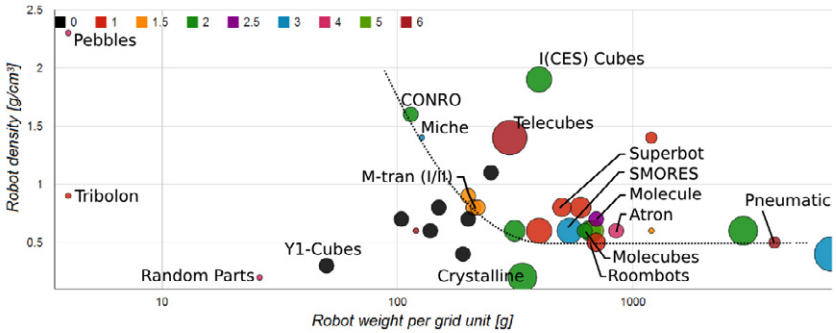

Fig. 2. Graphical presentation of the robot density of 34 modular robot systems. A more comprehensive robot list can be found in Table A.2. *x*-axis values show the weight of each robot normalized by the number of grid units it occupies. RB for example occupies 2 grid units and weighs 1400 g, hence 700 g is plotted. Robot density is shown on the *y*-axis, also normalized per grid unit. Since RB uses a $11 \cdot 11 \cdot 11$ cm grid, a density of 0.5 g/cm^3 is assigned. Bubble sizes increase with the number of active joints per module per unit grid (RB has 1.5 joints per grid unit, Telecubes features six actuators). The number of active connection mechanisms (ACM) per unit grid is color coded, RB features one ACM per RB grid unit. Very small data points indicate modular robot systems with no active joints; these are typically stochastic modular robots. Black-colored data points classify modular robots with no ACM. Often chain-like modular robots are connected manually. The dotted line on the right part of the figure indicates a lower bound of density, valid for most ACM- and actuator-equipped modular robots. (For interpretation of the references to colour in this figure legend, the reader is referred to the web version of this article.)

connector ports. *Multi-mode* [14] locomotion types are possible, such as legged locomotion, caterpillar-like locomotion [15], or modular robots transforming into a wheel [14] and using rolling motions. *Bipartite modular robots* (e.g. M-TRAN III, [16]) use two different sets of connection mechanisms within one module class. A female and a male set of connectors can be used, because bipartite systems move typically within a 2D or 3D checkerboard grid. This feature of bipartite systems can reduce their cost and complexity. If a modular robot system is *not* bipartite but any module part can show up at any place on the 3D grid, an ACM design with *hermaphrodite* (genderless) characteristics can avoid a potential connector mismatch. By allowing wheeled or track-mounted robots to connect to each other, *mobile modular robots* are created. As a collective, they can overcome obstacles that are larger than a single unit (e.g. Swarm-bots [17]). *Hybrid modular robot systems* can include features of all the above systems.

In Table A.2 we have listed 72 modular robot systems, created since 1988 [18]. From 34 of them we were able to identify the module's weight, unit grid volume, number of active connection mechanisms and number of active DOF. In a few cases we used approximations to fill up missing values. We normalized the modules weight *per unit grid*. This is meant to make MR systems comparable, since some occupy a single grid unit, and others span over several grid units. Robot density was calculated as the density of the robot within the entire grid unit volume, not only the volume capture by the robot's shell. Normalized robot mass is plotted over normalized robot density (Fig. 2), and the *x*-axis is plotted on a log scale, due to the large range of different MR systems. Data point bubble sizes indicate how many active DOF a module has per unit grid (from 0: e.g. Random Parts modular robot [11] to 6: Telecubes [19]). The smallest bubble sizes indicate no active degree of freedom. Those MR are often stochastic modular robots, propelled by their environment. Bubble colors indicate the number of active connection mechanisms per unit grid. MR systems labeled in black apply passive or manual connection mechanisms, with no active connection mechanisms. A lower limit in normalized robot density in the full range of mass can be found, below a density of 0.5 g/cm^3. More dense packings indicate more features, such as stronger actuators and gearboxes, multiple sensors, many active degree of freedom, or a heavier shell design. However, the modular robot's normalized density will influence its performance if modules have to be lifted, and if they are connected in-series. Joint torques are the result of lever length and effective lever angle, versus weight of the lever and direction of gravity. With the task of handling modules and objects, a balanced modular robot design with many features and a *low normalized robot density* is an advantage. MR systems span a large range of weight, from less than 4 g (Tribolons, [20]) to several kilograms per robot per grid unit (3D-Unit, 7 kg [21]). Extremely light-weight MR have typically a simpler design: fewer or no ACM or active joints. The majority of modular robots ranges from 0.1 to 1 kg. A possible explanation can be the size of portable and non-portable actuators (electrical, magnetic, pneumatic), nowadays battery technology, and the state of current rapid prototyping techniques. The latter was very influential in the design of Roombots. Many MR platforms apply printing technology [22–24,16] during their production.

If we remove from Fig. 2 all MR systems without an active degree of freedom (smallest bubbles), and all modular robots with no active connection mechanism (black bubbles), then the remaining SR-MR are placed above a minimum density (0.5 g/cm^3, dashed line, Fig. 2). Only two MR systems, the two-dimensional Crystalline robot [25] and the very large 3D-Unit have a lower unit density. For normalized robot weights of less than 0.2 kg, the unit density increases even further. This lower bound is an observation among current, fully self-reconfiguring modular robots. It could indicate that to build a fully equipped SR-MR, complexity and self-sufficiency is being "payed" by a module density of above value. If the task of a MR system is similar to our Roombots scenario, and involves handling of modules, brachiating, and handling objects, then a higher normalized unit density size is a disadvantage. Fig. 2 indicates that the currently observed lower bound is dependent on the MR unit-module size, and increases with decreasing module size.

For a full-lattice modular robot, Roombots has a comparatively low normalized robot density (0.5 g/cm^3), a relatively large grid unit size with a grid cube edge length of 110 mm, and a grid cube weight of 0.7 kg. These parameters are the result of pushing for a light-weight construction with three powerful joints. RB can lift four robot grid units (one full metamodule) in any orientation. For comparison, the strongest modular robot (Polybot, Yim et al. [7]) can lift five unit grids, one more than Roombots. RB weighs 1.4 kg, has two of its ten available connector sockets equipped with active connectors, and features a full set of electronics and batteries. We find that, in our scenario, a larger grid cube size and many available connector ports are well suited to build on a macro-scale. The large choice of MR systems and solutions (Table A.2) and their capabilities, characteristics, and restrictions (Fig. 2) indicate the importance of a careful design process for a new MR system.

3. Material and methods

This section gives details of Roombots' mechanical design (Section 3.1). This includes its active connection mechanism (ACM), actuator design, and shell and grid design. Section 3.2 presents Roombots' electrical components. Section 3.3 describes control schemes for distributed locomotion, and reconfiguration.

3.1. Mechanical hardware

This section provides hands-on details on the Roombots hardware design and design process, its active connection mechanism, actuation, and shell design. A brief description of the passive grid design is included.

Active connection mechanism. Roombots' active connection mechanism design was loosely inspired by the AMAS [1] ACM based on physical latches, and has been adapted and evolved for Roombots' needs. Our requirements for a connection mechanism, through the application of RB in our daily living environment, were rather strict; a list is added in this section. This list ruled out several early design options. We excluded high-voltage surfaces and latching principles which required an external power supply or other non-internal means of force transmission, such as pressurized gas or fluids. Initially we excluded static or switching high magnetic forces, as they might damage storage devices. However, we later chose to test a hybrid ACM design, and found very good results. Therefore, we will later also present one experiment with a hybrid gripper-magnetic ACM. Recently a number of novel connection mechanisms have been developed, which are based on material connections, rather than frictional connections. Neubert et al. [26] introduced a connection mechanism for self-assembly in a fluid tank that applies melting and solidifying of a low-melting point soldering material: Field metal. Revzen et al. [27] applied rapidly solidifying foam to connect internal MR components; this could also be extended to connect entire MR modules. Miyashita et al. [20] froze water between two neighboring connection plates with the help of Peltier elements. The ice bonds the two neighboring modules together. Wang and Iida [28] used hot-glue to connect MR robotic elements. The glue connection can be reversed by reheating the bonding layer. The aforementioned techniques are still at a prototyping stage. For Roombots' ACM, we were looking for a reliable, low energy consuming connection principle. Eventually, connection principles based on electromagnetic forces, electrostatic forces, hydrostatic pressure, hydrodynamic forces, and atmospheric and vacuum pressure were set aside in favor of a connection mechanism based on physical latches. Roombots' ACM needs to provide the following features: (a) *Locking of all degrees of freedom*: No translation or rotation is allowed after connection. The entire mechanism should be very stiff, to reduce bending of the RB structure. (b) *Passive guidance*: We were aiming at using the latches and/or the connection surfaces to guide the connection procedure. Zykov and Lipson [9] shaped connection surfaces to guide approaching modules in a fluidic environment. Vona et al. [29] designed very large grippers, which robustly connected the robot to truss-structures. (c) *Stiffness and size*: By studying e.g. the active connectors of AMAS [1] and ATRON [13], one can identify that the connection mechanism should be small enough to easily fit into a modular robot, and still leave space for actuation, electronics, and batteries. It should also rigidly integrate into the RB shell, such that it will not weaken the module's overall stiffness characteristics. (d) *Grasping range* can help to increase the robustness of the connection process. Fig. 5 depicts four principles; based on a pin-and-socket system, a simple rotating hook, the AMAS ACM, and the RB ACM. The AMAS and the RB ACM are complex, but also compact. The RB connection mechanism was designed to produce a scooping movement which pulls the neighboring module towards itself. Potential misalignments (parallel distance up to 3.5 mm) between modules can be self-corrected by this scooping movement. A basic hook design (Fig. 5(b)) also applies a scooping movement. However, the analysis of the hook design shows that separating forces between modules apply an opening torque to the gripper. (e) *Groove shape*: Often connection robustness is increased by providing a special groove design, (Fig. 4(b), left and right of the black latches). Around 2 mm of misalignment in sideways directions are compensated by Roombots' ACM groove design. (f) *Symmetry, gender, and bipartite systems*. RB is a homogeneous MR system, with an ACM that can connect directly to any other RB ACM, but also to a passive connection port. It has male and female connector features within one ACM: latches and grooves (hermaphrodite ACM). A bipartite system, such as Molecules [30], has latches and grooves separated. (g) The *latch and groove* design allows one to design flat connectors, and the absence of pins or other extrusions allows a relatively smooth surface design. Hence, we can easily integrate non-actuated connector plates of Roombots' ACM into the floor, wall and ceiling. A simple connector surface characteristic is also helpful for furniture design. (h) A *compact, flat, and wide design* is advantageous for equipping a modular robot with several ACMs. We found through testing and experimentation that it was sufficient to equip only two of ten available Roombots module sockets with ACMs, for all the shown tasks in this work. This is also possible because of Roombots' three DOF: they allow any mounted ACMs to swivel to any socket position in its unit grid. If we encounter cases where more ACMs are required then we can equip sockets accordingly. Especially for the full Roombots scenario, where RB modules are tightly packed into structures together with lightweight, structural elements, more ACMs will become important, to strengthen the connection and stiffen, for example, the table structure (Fig. 1). (i) The *power consumption* of an ACM must be minimal, by applying power only during the change of connection mode. For example, using frozen ice as a bonding material [31] requires constant cooling to keep the connection. Roombots' ACM requires no power in the connected state. Its crank and slider mechanism (Fig. 4(a)) pushes the latch into an externally non-reversible singularity position. Roombots' ACM has a weight of 57 g, including actuation, mechanical elements, and the electronic control board. It is 65 mm in diameter, and between 19 mm (without motor) and 32 mm (with motor) in height. A 150:1 geared motor (#21, Fig. 4(a)) actuates a drive chain of three plastic spur gears (#26 #18 #5). A crank (#15) and slider (#9) move the latch (#10), which rotates around two axes (#11 #27).

Module degree of freedom. When we chose the Roombots' degree of freedom type, we searched for a design which could maximize the number of ACM per module. The Molecubes [32,22] DOF design offered the most connectors (six) for a regular cubic grid, by using a diametrical DOF. However, a modular robot occupying a single grid unit is less potent for self-reconfiguration on-grid, at least two coupled DOF spanning over two grid units are required. Examples for such paired MR are M-TRAN [33] and SuperBot [34]. RB are designed with three continuously rotatory degrees of freedom (Fig. 3). We chose to implement a system with two outer, diametrical, Molecubes-like DOF. In Roombots, we connected the two outer diametrical DOF by a central, continuously rotatory DOF, similar to SuperBot's center DOF. This outer–central–outer DOF design allows Roombots to approach a concave edge, by freely choosing the required orientation of its two diametrical DOF (Fig. 8).

Eventually, Roombots combines wanted features from at least three SR-MR: Molecubes, and its continuously rotating active degree of freedom and many available sockets, Superbot with a center joint between a module spanning over two grid units, and

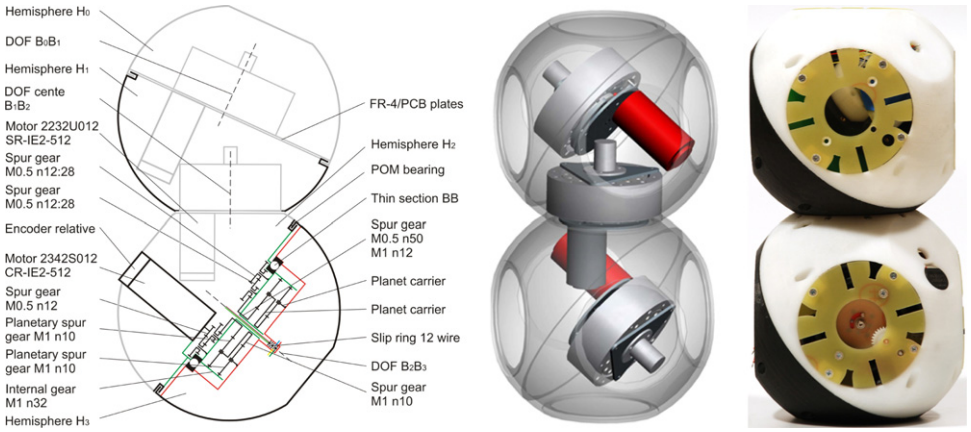

Fig. 3. Left and center: Schematics of the gearbox and shell mechanics of a single Roombots module, one of three joint actuators is depicted in detail. Active connection mechanisms (ACM) and passive connector plates are omitted. Right: picture of a full Roombots module. The lower frontal connector is a fully equipped, active connection mechanism. The upper frontal slot is equipped with a passive connector plate.

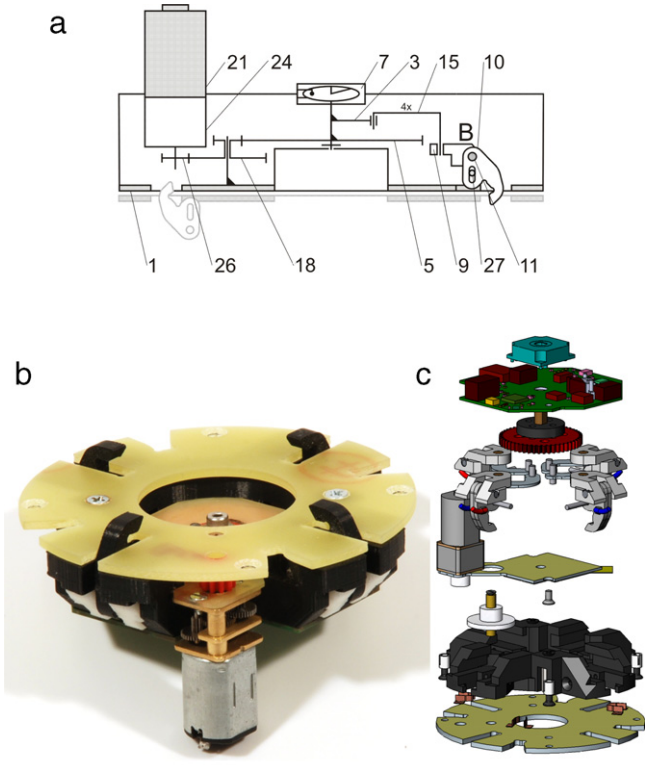

Fig. 4. Roombots (RB) active connection mechanism (ACM). (a) Schematic presentation of its mechanical gear train. (b) Photo of the real mechanism. (c) ACM explosion view.

M-TRAN [33], which applies a module design with a pair of joints distributed over two unit grids.

To create a Roombots half shell, the common volume between a cube with an edge length of 0.11 m and a sphere with a diameter of 0.128 m is cut in half (Fig. 6). Four of these half-spheres create one RB module. RB has no joint limits, all DOF can turn continuously. This allows for a highly versatile grid based locomotion (Section 4). We found that continuous joint rotation is very helpful during reconfiguration, because a choice of direction, clockwise or counter clockwise, is available. Roombots' rounded shell shape is well suited for human–robot interaction. Half-spheres can further be used as wheels (see Section 4.1).

Actuation. Roombots' degrees of freedom allow for not just oscillating, but also continuous rotatory movement. Roombots' outer shells can be used as wheels. After locomotion, the second major task of RB is self-reconfiguration and locomotion through self-reconfiguration. Any of the three Roombots' joints needs at least to be able to lift the weight of a single module, and a second attached module (four grid units, see Section 2). To fit this actuator requirement, we implemented a custom-designed gear train, where we choose plastic spur gears with low weight and a large gear module. The gearbox aspect ratio is wider than it is high (Fig. 7). The gearbox is light-weight, compared to commercially available spur or planetary gear trains of similar size.

The weight of one RB module is 1.4 kg, its center–center length is 110 mm, the overall length is 220 mm, and its outer dimensions are 110 mm × 110 mm × 220 mm. Approximately, the required torque for lifting a stretched metamodule from a horizontal position is 2.5 Nm for the center joint and 4.9 Nm for the outer joints. Brushed motors (M_{center} = 0.048 Nm, M_{outer} = 0.08 Nm stall torque, Fig. 3) drive an initial spur gear train. This first stage provides a gear ratio of ≈27:1. An in-series double planetary gear stage increases the gear ratio by a factor of 13.5 and the total gear ratio is 366:1. Neglecting losses, which are between 5% and 10% per gear stage, a stall torque of M_{center} = 17 Nm and M_{outer} = 29 Nm is available. This actuator design proved to be sufficient to rotate a full RB metamodule from any position, at reasonable speed. To lift up heavier objects, such as a third module at the end of a metamodule, and with full lever length, the current actuator design would be too weak. For this reason, and because long-levered, in-series manipulators show large uncontrollable deflection, we currently envision two metamodules handling objects in cooperation (Fig. 1, F2). The case of multiple Roombots metamodules handling passive objects in cooperation has not yet been researched, and presents one of the remaining challenges of the full Roombots scenario (discussed in Section 5).

Shell design. RB shells are 3D printed from acrylonitrile butadiene styrene (ABS) plastic (Fig. A.21), keeping the idea of rapid manufacturing, scalable production, and multiple design iterations in mind.

Early RB prototypes [4] showed large module deflection under load. We identified that the module design as a sum of in-series coupled ABS half-shells, active and passive connector plates, and joints was of too low a stiffness [35]. This prevented RB prototypes from successfully mastering, for example, the wall-climbing task. We introduced two major changes to increase the stiffness of a single RB module.

We replaced the previous RB single-hull shell design (Fig. 9(a)) with a hull–rib–hull design (HRH, Fig. 9(b)). The larger cross-sectional area of the HRH-shells provides an approximately double

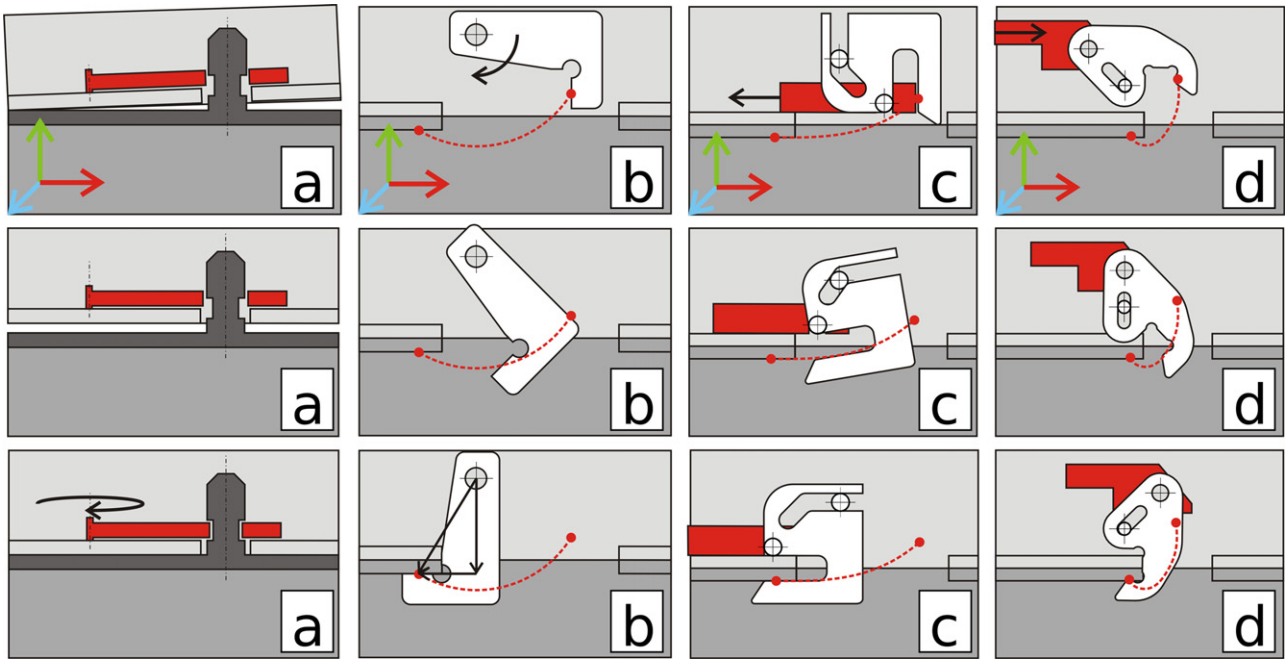

Fig. 5. Four different active connection mechanism principles, based on mechanical latching. (a) Pin-and-socket, (b) simple rotatory hook, (c) AMAS [1] connection mechanism, (d) Roombots active connection mechanism.

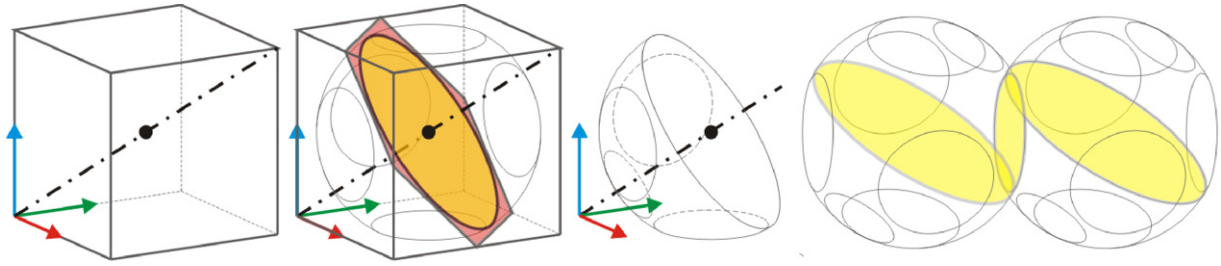

Fig. 6. Creation of Roombots half-shells. Four half shells build one 3-DOF Roombots module. The diametrical degree of freedom (left image) was first applied by the Molecubes [22] modular robot platform.

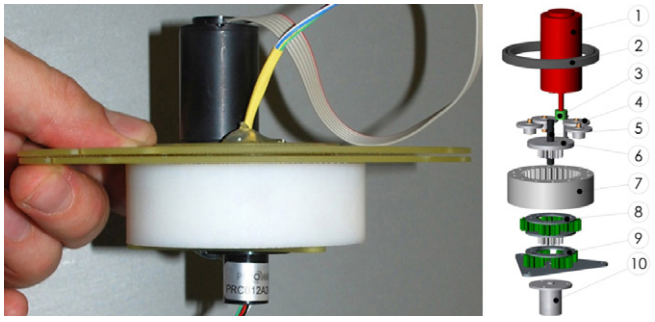

Fig. 7. Roombots' gearbox design. A brushed motor (1) drives an initial drive-chain of spur gears (3–5). A second set of planetary gears (6–9) increases the available torque further. A slip ring (10) provides power and communication at continuous joint rotation.

shell stiffness. These results were gathered with the help of finite element analysis (FEA) of a simulated RB module, applied in Solidworks (data not shown). Although the shell is stiffer, its weight was kept mostly constant through its hollow-wall design. A disadvantage of the new design is less space within the modules.

A big difference was made by a set of custom designed, large-diameter POM bearings between two RB hemispheres of the same module (Fig. 3, left). Earlier RB designs applied a single, small-diameter metal ball bearing at the DOF center, and bending affected the fiber glass sheets between the half-spheres. Both changes, plus further material and parameter adjustments on the ACM latches, were required to successfully run *3D* grid-based locomotion and reconfiguration experiments. Robustly connecting ACM are necessary, and have to be supported by the entire RB module. The RB hardware configuration presented here could robustly perform the presented subtasks (1–5). Important, currently infeasible subtasks include on-grid locomotion of metamodules (as opposed to single module on-grid locomotion, which works well) and cooperative RB metamodule handling of light-weight, structural elements. For these subtasks the current RB metamodule shows too large a deflection, and prevents open-loop grasping of the end-effectors.

Building materials. At the initial design phase of a modular robot system, it is hard to estimate the final weight and volume distribution. Values for Roombots are provided in Fig. 10, for a Roombots module with a mass of 1.4 kg. ABS pieces provide a quarter of the robot's mass and half of its volume (Fig. A.21). The sum of Roombots' frame and its ACMs is composed of ABS pieces, glass fiber plates, milled POM pieces, and three off-the-shelf steel ball bearings. This accounts for more than half of the robot's mass (65%, 0.72 kg) or 82% of its rigid volume. Using ABS is easing the RB production. At the same time, 3D printed ABS is less rigid and of lower quality than molded ABS. Therefore, the Roombots HRH shell design was helpful to improve the ABS shell stiffness.

Grid design. For the grid implementation (*structured* environment), we directly reused the connector layout, which we fused with the

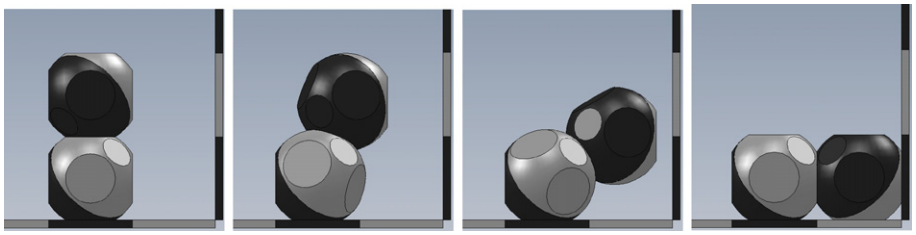

Fig. 8. Roombots module approaching a perpendicular wall (concave corner). The module is placing its connector parallel to the wall of this concave barrier by rotating its three joints simultaneously.

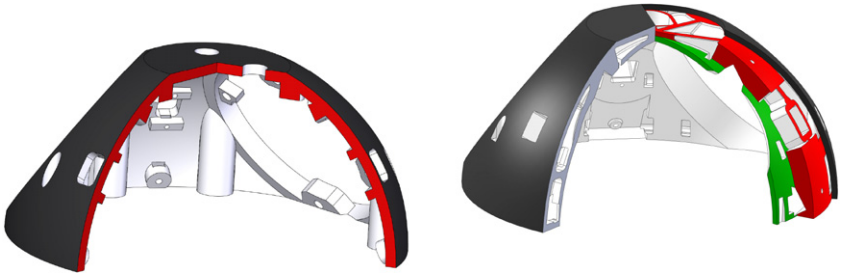

Fig. 9. (left) Partial cut-view of the earlier RB shell design, with a single-hull layer. (right) Cut-view of the upgraded shell design, a hull–rib–hull (HRH) construction. With the new hull design, the shell weight was kept low, the cross-sectional area was increased, and the shell was stiffened by a factor 2. The HRH shell design also slightly reduced the available space inside the modules.

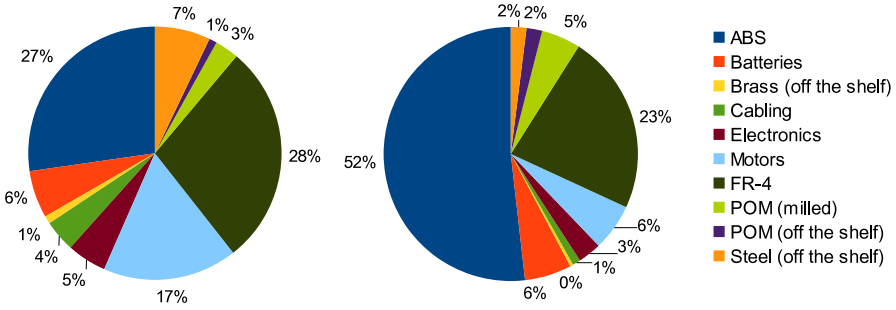

Fig. 10. Mass (left) and volume (right) distribution of mechanical and electrical components within one RB robot. Volume is measured per volume of rigid components. The distribution of rigid parts versus empty volume is roughly 35:65, respectively. (For interpretation of the references to colour in this figure legend, the reader is referred to the web version of this article.)

grid connector plates. These grid plates are placed on a wooden frame equipped with recesses made for Roombots' grippers. To be compatible with Roombots' ACM, grid plates must have the same thickness as the RB connector plates (1.5 mm). Fig. 18 shows two RB modules handling two grid plates. Each grid plate has four integrated docking ports and the outer plate dimensions are 220 mm · 220 mm · 1.5 mm.

3.2. Electronics hardware

RB modules have full computational, energy, and actuator autonomy. Each RB module includes a set of modular electronic boards (Fig. A.19), with motor boards (MB) for main joints and active connection mechanism actuation, power management (PB), and wireless communication (Bluetooth board: BT). RB modules can be powered both from an unregulated, external power supply, or a set of internal batteries. We are currently using a 4-cell (4S-1P) Lithium Polymer (LiPo) battery pack (BAT, Fig. A.19) with a capacity of 910 mAh. LiPo batteries do not provide a constant voltage. The output voltage of a single cell varies from about 4.2 V to 3.0 V, therefore the output of the RB battery pack varies from 16.4 to 12.0 V. The power board protects the batteries from discharging below 12 V. It further generates two supply voltages for the RB electronics: (1) The main motor supply is generated through a single ended primary inductance converter (SEPIC, LT3757 [36]). It can both boost and step down the battery voltage and provides a stable 15 V supply (black lines, Fig. A.19) with a continuous output current of at least 5 A. (2) All other electronics and ACM motors are powered from a 6 V supply (red lines, Fig. A.19). This voltage is generated by a step-down converter (LT3680 [36]), with a continuous output current of up to 2 A. In its resting state, RB modules consume 350 mA, allowing the module to stay active on battery for roughly 2 h.

Communication and power are transmitted within the modules through slip rings, which allow continuously rotating joints. Intra-RB communication is realized by a half-duplex RS485 communication bus (green lines, Fig. A.19). We chose RS485 as the physical communication layer as it is based on differential wires. This makes the communication robust against noise. RB communication has been tested and been found well suited for transmission through the module's slip rings. Integrated RS485 driver circuits (ADM3078E [37]) can directly be connected to the universal asynchronous receiver transmitter (UART) interface of a microcontroller. In combination with the 40 MIPS dsPIC33 microcontroller (dsPIC33FJ128MC802 [38]), raw data rates up to 10 Mbps were reached. In practice, a 115 200 baud rate was sufficient.

Inter-module and PC-to-module communication was realized by a wireless Bluetooth link. The communication board (BT, Fig. A.19) features a Class 1 Bluetooth module (WT11-A [39]). It supports data rates up to 550 kbps. The Bluetooth link was used

Fig. 11. First off-grid Roombots metamodule (MM) locomotion type: MMs use the module's outer spheres as wheels, only two of six joints are active. The distance between light-green marker lines is 0.5 m. The maximum continuous locomotion speed was 13 cm/s, and the direction of locomotion is to the right. Marker lines on the floor were emphasized to identify module movement. (For interpretation of the references to colour in this figure legend, the reader is referred to the web version of this article.)

during the experiments to remotely control RB modules from a host PC.

Each RB degree of freedom is actuated by a brushed motor, controlled by a motor-driver board (MB, Fig. A.19). Each MB contains a dsPIC33 microcontroller running the software motor controller and communication protocol for the remote motor control. The microcontroller drives a brushed motor through a full-bridge PWM motor driver integrated circuit (IC, A3959SLP [40]). It takes the motor's relative position encoder signal as feedback for PID position and speed control. The processing power of the dsPIC33 was sufficient to further integrate a central pattern generator controller. The motor-driver board can provide continuous currents of up to 2 A.

The grippers of a Roombots active connection mechanism (Fig. A.19) are position controlled, using a PD controller with hysteresis adaptation. The controller is implemented on a dsPIC33 that drives the ACM brushed motor through a full-bridge PWM motor driver integrated circuit (A3953SLB [40]). It provides currents up to 1.2 A. The controller uses an analog potentiometer feedback, read by the microcontroller's analog-to-digital (AD) converter, with a 12 bit resolution.

Fig. A.20 shows the externally measured, instantaneous current consumption for a simple motion and connection/disconnection sequence: the ACM releasing the connection (1 J energy consumption), the RB module rotating to a vertical position (13 J), the module moving back to the horizontal (7 J), and the ACM closing (3 J). During normal operation, we measured a base power consumption of 5 W.

3.3. Control

RB modules can move in two basic ways: (1) Single modules and metamodules can move *on-grid*, via passive connectors embedded in floor, walls and ceilings and in other RB modules, through brachiating moves. (2) *Off-grid*: a structure made of RB modules can move freely by modulating its shape rhythmically, actuating the modules' main degrees of freedom.

To control RB to move on-grid through reconfiguration, we developed a reconfiguration software framework. To exploit the ability of single RB modules to autonomously reach any position on a 2D grid, we developed an online reconfiguration planner based on the $D^\star$ algorithm and motor primitives. This planner is closely linked to the RB hardware and allows one to control a Roombots module on a 2D grid by requesting a final reaching position [5]. The current implementation of our reconfiguration framework for controlling RB *metamodules* [41,42] takes inspiration from the work by K. Stoy [43].

Our off-grid locomotion control framework combines central pattern generators (CPG) with learning techniques [44]. CPG are networks of coupled oscillators producing rhythmic outputs without requiring a rhythmic input [3]. CPG are capable of generating robust and synchronized locomotion patterns with few control parameters. Those can be found using learning techniques. The distributed oscillators of a CPG can directly be mapped to the morphology of a modular robot.

4. Experimental results

To demonstrate the capabilities of the RB system, we conducted five main experiments. The results are presented in this section. The link to the video including all experiments can be found in Table A.1.

4.1. Off-grid metamodule locomotion

Roombots can be used to study both the reconfiguration and locomotion control of articulated robots. Here, we explored two off-grid examples of RB metamodule locomotion. With 6 degrees of freedom, RB metamodules can perform various types of locomotion.

RB joints are capable of performing both oscillatory movements and continuous rotation. Snapshots of a Roombots MM configuration exploiting continuous rotation are shown in Fig. 11. Two RB modules were joined and folded, and the outermost RB spheres were used as wheels. We controlled the speed of two of the metamodule's six joints, while four joints stayed still. The RB metamodule reached a maximum forward velocity of 13 cm/s. The direction of (wheeled) motion was easily controllable by directly setting a speed difference between the two active joints.

Snapshots of a gait where the metamodule's DOFs were controlled with joint oscillations are given in Fig. 12. RB joints were controlled with a network of six oscillators, coupled into a central pattern generator. Oscillators were implemented as a set of coupled differential equations [44], running on-board, and were solved with an Euler integration with a time step of 10 ms. This configuration reached a forward velocity of 4 cm/s at an oscillation frequency of 0.16 Hz. In Fig. 12, the metamodule is shown while passing over an obstacle with a height of 23 mm.

4.2. Reconnection of RB metamodules to the on-grid environment

We showed earlier that RB modules can locomote off-grid, if for instance no connector ports are available, or to reach a point on the plane rapidly. To connect a Roombots metamodule from off-grid to on-grid, its ACM has to be aligned to a grid element. We designed and implemented an entrapment mechanism [46] (Fig. 13) that helps to autonomously align and connect RB metamodules on-grid. The EM is a passive tool, and a metamodule has to provide its own actuation to reach it, slide into it, and go on-grid from there. The experiment (Fig. 13(a)–(d)) is a proof-of-concept of RB module realignment and on-grid connection. Physical intervention by the experimenter was not required, but RB modules are currently not equipped with sensing of their position and orientation in world-coordinates. Therefore a human operator remotely controlled the joint movements and ACM actions. We found that small joint oscillations helped to align the MM at the base of the EM. This also helped the ACM to grip the EM-port (number 5, Fig. 13(d)). In the future, the following steps will be required for an automatic module transfer from off-grid to on-grid: (a) The orientation of the metamodule after sliding into the entrapment is firstly unknown. Sensors will detect the MM's orientation, and guide further moves.

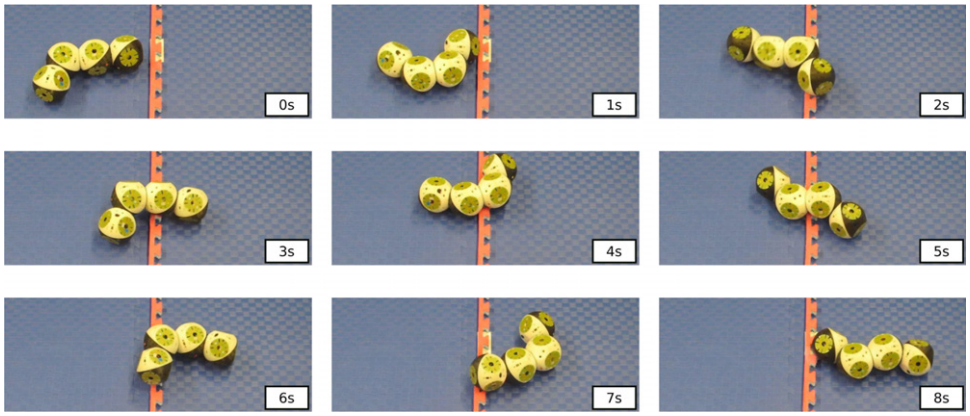

Fig. 12. Second off-grid metamodule locomotion type: it applied oscillating motions at four of Roombots metamodule's six joints. Joint motions were controlled by a network of coupled oscillators. On its way the metamodule overcomes a small obstacle (central red line) of 23 mm height (20% sphere height). These locomotion patterns moved the module to the right, with an average speed of 4 cm/s. (For interpretation of the references to colour in this figure legend, the reader is referred to the web version of this article.)
Source: Snapshots were taken from a movie [45].

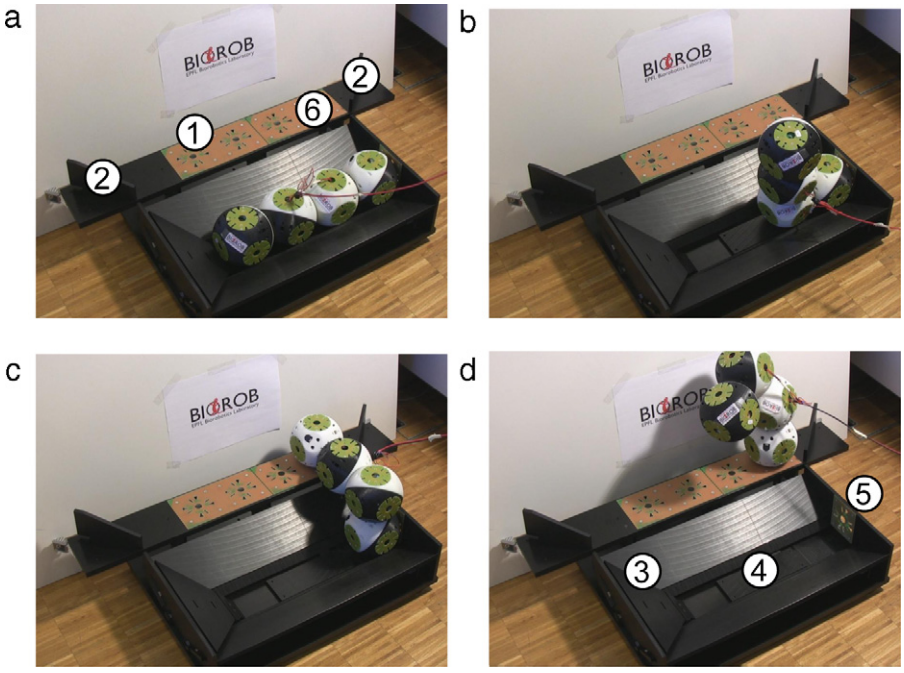

Fig. 13. Demonstration of transferring a Roombots metamodule from off-grid to on-grid. An off-grid moving RB-MM approaches the entrapment mechanism (EM) via point 1, and is guided through a set of walls (2) over a plastic slope (3) to the base of the entrapment mechanism (4). While sliding, it self-aligns with the entrapment. A vertical connection port (5) is mounted at the end of the EM. The MM locks itself to the port, and leaves the EM upwards, now on-grid (6).
Source: Pictures modified from [46].

(b) Currently, the elasticity and backlash of one metamodule (two-series coupled RB modules) is too large to autonomously and open-loop reach the goal connector on-grid. A human in the loop was required to remotely adjust joint movements. For an automated metamodule EM escape, we are working on a controller for elasticity and backlash compensation (control), and on stiffening the RB MM design (hardware).

4.3. Single module on-grid locomotion in 3D

This subtask illustrates the ability of a single RB module to autonomously overcome a concave edge and climb a structured wall. The setup (Fig. 14(a)) is composed of a horizontal and a vertical plate (of 2 × 6 and 8 × 6 grid units), shaping a concave corner. A single RB module starts on-grid, one grid unit away from the wall, and climbs the wall in 14 steps (Fig. 15), with four sub-sequences. (1) The approaching move towards the wall is a pre-computed, inverse kinematic (IK) based motion sequence (Fig. 14(a)–(c)). To avoid collision with the wall through the module's rotation, the approaching ACM is guided through IK based motion to stay parallel to the approaching wall. (2) Fig. 14(c): The module connects the wall approaching ACM, and disconnects its foot ACM. (3) Fig. 14(f): As before IK based motion was applied to avoid ACM–wall collision when rotating the module upwards. (4) A cyclic sequence of moves was used to climb the vertical surface. The RB DOF does not allow for a straight movement, but the module performed a zig–zag motion: right, up, left, and up (Fig. 15). Each move was followed by an ACM connection–disconnection. In Figs. 14 and 15 we show one RB module overcoming a concave edge and climbing a vertical grid wall. RB joint moves were executed autonomously, but we triggered ACM connections and disconnections manually. This ensured that a successful ACM connection had been established at every step.

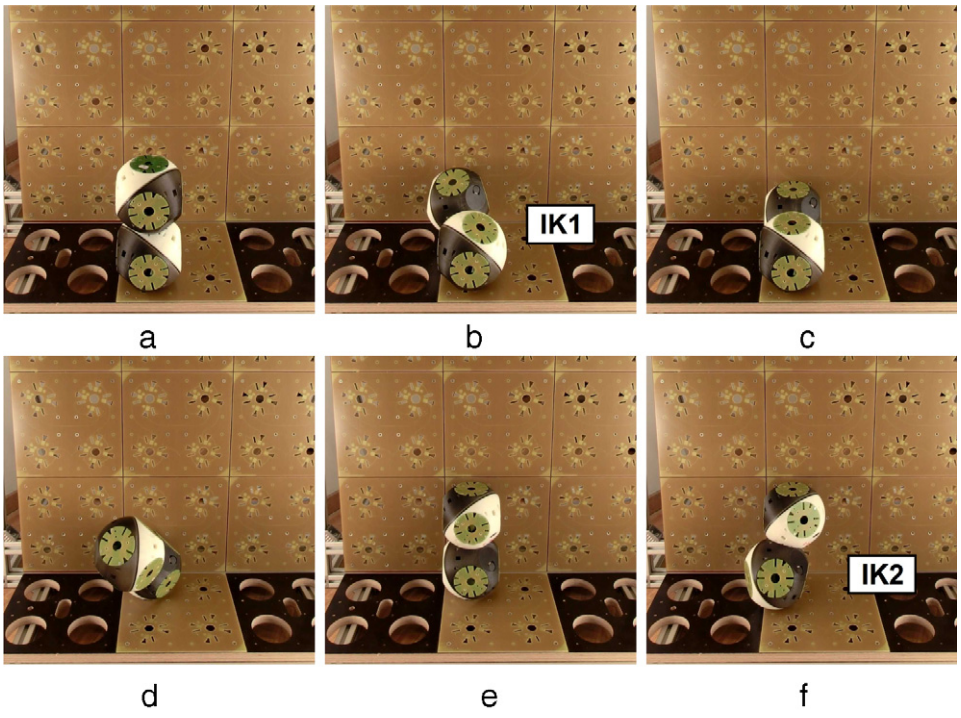

Fig. 14. A single RB module overcoming a concave edge. The initial configuration is shown in (a): the module is placed in its SRZ configuration and one grid unit away from the wall. (b) The module approaches the wall using inverse kinematics. In the connection phases (14(c) and (e)) always one ACM is first connected and then the second ACM is disconnected. (f) The module escapes the concave corner upwards.

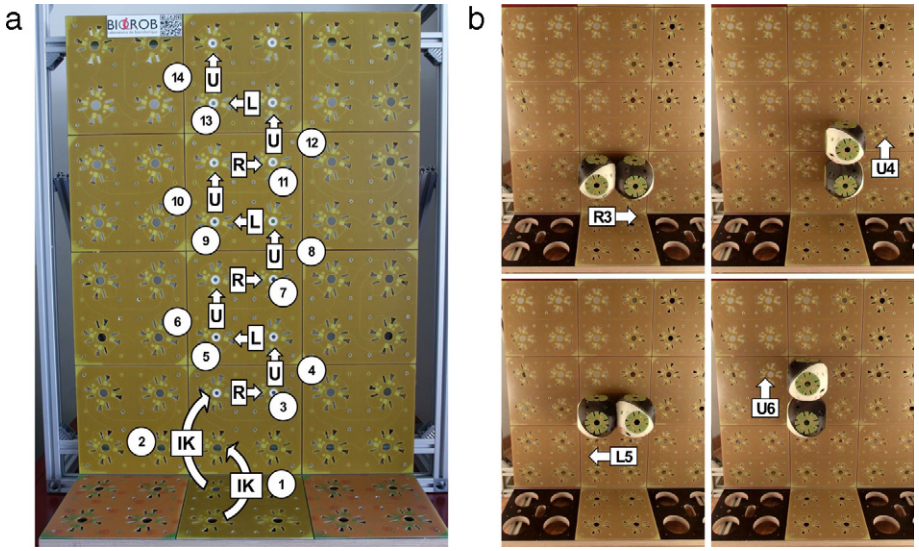

Fig. 15. (left) The sequence of 14 atomic moves used to climb the wall. *IK*: inverse kinematic based motion, *R* move to the right, *U* move up, *L* move to the left, in the global coordinate system. A connection and disconnection phase took place between each move.

In all above experiments we proceeded with an identical set of RB hardware: two RB modules, each equipped with two ACMs with mechanical grippers. Under standard laboratory conditions, such as module preparation, careful preparation of the on-grid plates and their connector ports, and constant module maintenance, the ACM gripping range of 3.5 mm was sufficient for all shown experiments. However, under rougher conditions, such as an open-day exhibition with many demo repetitions, we learned that the Roombots' purely gripper-based ACM required an improvement in gripping robustness. We observed that misalignment in connector port mounting and wear-out in the main gearboxes and ACM gripper mechanism lead to several unsuccessful connection attempts.

Therefore, we deviated from our very early ACM design constraint – not integrating a connector principle based on magnetic forces – and mounted a permanent magnet at the center of the gripper-based ACM and to each connector wall port. We experienced that this hybrid ACM – applying grippers to align, grip and hold, and the magnets to align – helped to dramatically reduce the number of unsuccessful connection attempts, after many experimental runs, and under rougher than standard conditions. We repeated the 14-step wall climbing experiment 15 times, and tested the robustness of the hybrid ACM. In 10 out of 15 trials the sequence was executed successfully in a completely autonomous manner. At four times the module had difficulties

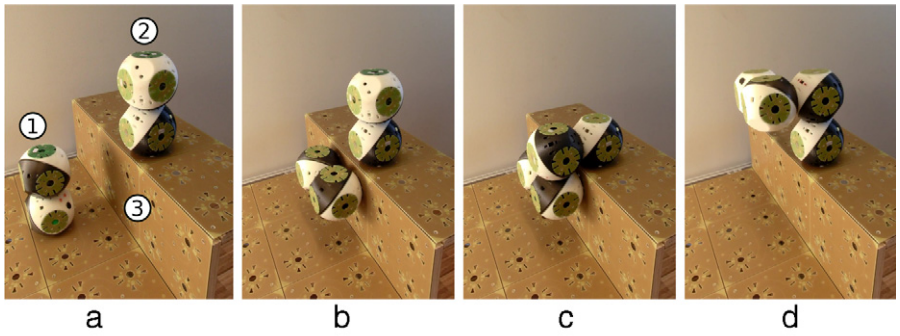

Fig. 16. A Roombots module overcomes a convex edge by joining with a helper module into a Roombots metamodule. (a) Module 1 (M1) is one grid unit away from the wall. (b) The module climbs the wall for one grid unit. (c) Module 2 connects its ACM to the approaching M1. (d) M1 is lifted onto the horizontal plane.

passing the initial concave corner, and was helped with a short human intervention by a small vertical force applied on top of the module. We identified a misaligned wall as the cause of this interference. Only once did the module systematically fail to connect after the *R* movement, and had to be helped. Those unsuccessful steps were not related to the grippers and we suspect a faulty joint sensor read-out. In sum, the hybrid ACM allowed very robust vertical wall climbing experiments.

If we continue using the hybrid ACM for the next generation of RB modules, we will exchange the centrally placed, fixed permanent magnet by a freely [4] rotating diametrical magnet, or a diametrical magnet with a small motor to turn, similar to the ACM design of Miche [47]. The tested hybrid ACM is in the current state not genderless, but the fixed-mounted magnets' polarity requires a magnetically matching counter port. The experiment in the next section again applied Roombots' standard, hermaphrodite, gripper based ACM.

4.4. Two Roombots modules join into one metamodule—crossing convex edges

This experiment demonstrates the ability of a Roombots module to overcome a convex edge with the help of a second module, and the ability of RB modules to join into metamodules. We showed earlier that single RB modules can overcome concave edges. To overcome a convex edge, a single RB modules requires the assistance of a second module. This is a kinematic constraint: the shortest distance from one connection port on the wall, over the convex edge, to the next port on the above plane is three grid units. Single RB modules are only two grid units long. The experimental setup was composed of three grid planes forming a concave/convex edge (#3 Fig. 16(a)). Two untethered RB modules: M1 and M2, were used. M1 was placed on the lower plane, and M2 "waited" on the upper grid plane. To approach and climb the wall, M1 performed the same motion sequence as in the concave-edge experiment (Fig. 14). Once M1 reached M2, both connected (Fig. 16(c)) into a metamodule. The MM lifted itself over the convex edge (Fig. 16(d)).

4.5. Manipulation of passive grid elements—building a table

In this example, two Roombots modules handle light-weight elements, and form a very simple table-like structure. Both RB modules grab their own passive, light-weight plate (connector port plate), lift it, rotate it, and form a table-like structure with a series of simple joint motions. In the experiment, both modules started on a horizontal grid (Fig. 18). One edge of the to-be-lifted grid plate (c_1 and c_2, Fig. 17) was rounded, to prevent collision with the underlying support structure during lifting. Module positions and lifted tiles are shown schematically in Fig. 17, while pictures of the setup are shown in Fig. 18.

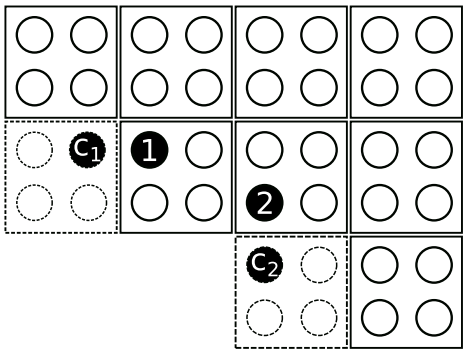

Fig. 17. Schematic view from the top of the setup used during the light-weight element manipulation task. Module 1 (M1) and module 2 (M2) are represented by filled, numbered black circles. c_1 and c_2 are passive connectors to which M1 and M2 attach, respectively. Dashed tiles are the to-be-lifted, light-weight elements.

5. Discussion and future work

The presented hardware experiments show the capabilities of the current Roombots generation. These experiments also reveal the remaining challenges for the full, envisioned Roombots scenario. We successfully demonstrated that RB modules autonomously move on a 2D grid, overcome concave corners, form metamodules, and cooperate to overcome convex corners in a structured 3D-grid environment. We presented a proof-of-concept showing how RB modules can handle passive, light-weight parts. An entrapment mechanism makes it possible to realign RB metamodules back on-grid, after off-grid locomotion.

The challenge for the presented experiments was a Roombots module design and implementation that worked reliably in the presence of module and docking port elasticities, and material and production tolerances, such as gear backlash. At the same time, module weight had to be kept low. It was also important to provide sufficient torque to move RB metamodules, and enough joint velocity to reconfigure and move with a reasonable speed. While an earlier RB prototype generation already worked on horizontal grid planes [5], climbing vertical walls, overcoming convex corners, and joining Roombots modules in 3D into a metamodule was so far not possible. The stiffness of earlier RB prototypes was too low, because of the in-series structure of RB half-shells (single-layered ABS), small-diameter ball-bearings, weaker joints, and RB connectors. This led to a module deflection larger than what the ACM latches could compensate for. To be able to run all five new experiments, we solved this issue by (a) stiffening the RB shells, (b) introducing large, custom bearings to stiffen the RB joints and (c) modifying the materials, tolerances, internal friction, and ACM latch parameters. Printed ABS shells are less stiff than molded or metal ones. Nonetheless, we kept ABS as the main shell material. 3D-printed ABS pieces enable us to cheaply and

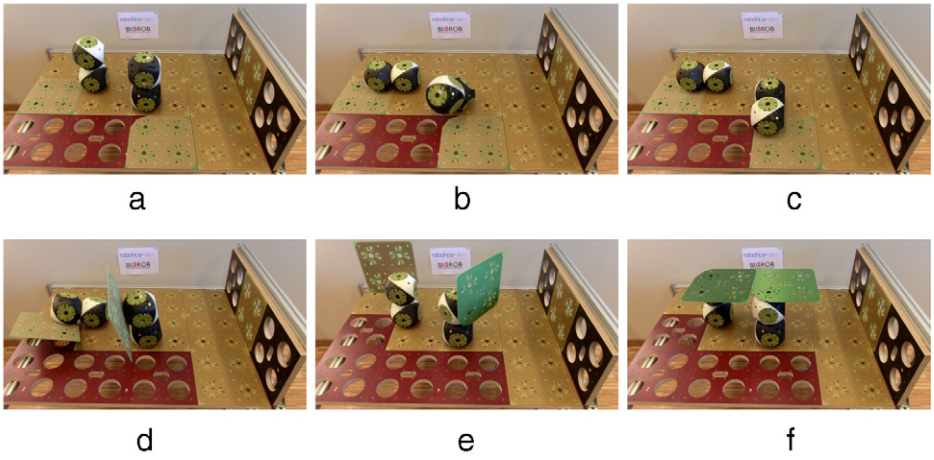

Fig. 18. Simple example of two RB modules handling passive structures. Modules picked up two plates and aligned them into a small table-like structure. (a) The initial configuration of the modules and the passive plates on the 2D grid. (b) Modules were leaning down. (c) Connection phase during which modules use their free ACM to pick passive plates from ground. (d) Lifting phase. (e) Intermediate state during the orientation phase of the plates. (f) Final module configuration with lifted plates. Our full Roombots scenario will require very much more complex handling procedures, including cooperative, parallel handling of structural objects by several RB modules.

rapidly redesign and build modules which are very compact and light-weight. The ACM latch scooping movement is 3.5 mm deep, more than double the thickness of the connector plates, and compensates misalignments in this range. We experienced that permanent magnets at the center of connection ports improved latching robustness further, in combination with the latch grasping movement. This hybrid ACM design counteracted module wear and enabled on-grid locomotion in a somewhat "flawed" (and more realistic) grid environment.

A future challenge will be on-grid locomotion with a meta-module, instead of multiple separated, single RB modules as we are currently showing here. Metamodules could potentially reach more remote positions in the 3D grid, and could handle objects freely over distances. However, the long-lever, in-series structure of a metamodule deflects significantly under gravitational forces. While we were able to improve the stiffness of Roombots modules, for example through a double hull shell design, a current generation fully stretched Roombots metamodule will not reach precisely, repeatably and open-loop a goal connector, while single RB modules robustly succeed in this task. We plan to use external sensor information to locate nearby ports, and to estimate and compensate for metamodule deflection. We are working on adapting technological and manufacturing advancements, such as direct metal deposition printing and carbon fiber reinforced shell parts. These should make it possible to replace ABS shell elements by equally light-weight parts, but with significant higher stiffness.

In a few experiments visual human guidance was required to compensate for elasticity and backlash effects, or to determine in which orientation a module landed in the entrapment mechanism. We will integrate off-the-shelf accelerometers, allowing RB modules to autonomously detect their orientation with respect to each other and within the grid environment. Absolute encoders will detect joint backlash, and infrared sensors will give a distance and alignment estimation of Roombots' ACMs. External sensors such as the MS Kinect can provide a knowledge of the environment.

We believe that larger RB structures are best built from a mix of RB modules and light-weight elements with embedded docking ports. Despite the compact RB design, modules currently lift little more than one additional RB module, in sum one RB metamodule. To lift heavier loads (full Roombots scenario) several RB modules will have to cooperate, and possibly also receive an actuator update. Cooperation of modules will create closed kinematic chains. To simplify the cooperative handling of structural elements, both mechanically and control-wise, we plan to insert "loose" joints, i.e. universal, passive joints connected in-series.

Through analyzing examples of self-reconfiguring MR, we have an estimation of the normalized module density of many MR and SR-MR systems (Fig. 2). This indicates to us that decreasing the normalized module density, while preserving module complexity, will be a challenge. But the analysis can guide us to optimize the gear ratio, motor size, and module's shell design. Advancements in portable electronics might help to reduce Roombots' power consumption and the weight of the electronics.

Both reconfiguration and locomotion experiments demonstrated that RB modules benefit from their configuration of three continuously rotating joints, with no joint limits. Roombots inherited its outer joint orientation from the Molecubes modular robot [32]. By choosing a module design ranging over two grid units, like M-TRAN [48], we reduced the mechanical complexity of the Roombots design: only a single ACM per unit grid was required for all presented experiments. ATRON modular robot [13], for example, rigidly integrates its ACM into its structure. This design proved to produce a very stiff module, but it would be hard to remove unnecessary ACMs. Fewer ACM per unit grid lead to a lower robot weight: RB have a normalized density of 0.5 g/cm^3. With two outer diametrical DOF, RB have five available connector ports per grid unit, and ten connector ports for the full robot. All of Roombots' faces can be used as attachment ports to assemble structures. Designs with non-diametrical DOF (M-TRAN [48], SuperBot [34]) have three connection ports per grid unit. In the case of ACM configurations with male–female characteristics, connection ports have to be matched to connect. Roombots' latch-based ACM is hermaphrodite and can connect to passive module ports, ACMs, and ports in the environment.

Roombots' unique and novel feature combinations, its adapted shell design, a strong, hermaphrodite ACM, a custom made, light-weight gearbox design, and a robust electronic backbone with multiple slip-rings enabled it to run successfully many different sub-scenarios of our full Roombots scenario. This included reconfiguration on-grid of single RB modules into RB metamodules, simple handling of light-weight objects, single RB module locomotion on-grid and in 3D, and off-grid locomotion of RB metamodules.

The currently explored direction of our Roombots design, towards the goal of a full Roombots scenario, such as the assembly of large structures such as a table, allowed us to identify the following remaining hardware and design challenges: (a) Roombots modules will require a stiffer construction and assembly of their structural components to achieve, for example, RB metamodule locomotion on-grid (future subtask F2, Fig. 1); i.e. the assembly of its

shell, joints, and active and passive connectors. We are planning to introduce a highly stiff structure (e.g. carbon-reinforced shell components) and stiffer connections between RB's structural elements. A low-weight, low density structural design will remain a strong RB design constraint. (b) Stronger actuators, at equal weight. The current RB metamodule can move itself around in 3D, in any orientation, at relatively high speed. To lift and manipulate larger structural elements a stronger actuation is required, and we are planning to optimize the motor–gearbox train towards a high efficiency, lower speed, higher torque configuration. According to our observations (Fig. 2), increasing the output torque while increasing the weight of the RB modules is suboptimal, as the module's unit density will increase. (c) We found that for *all presented* experiments two active connection mechanisms per RB module were sufficient. Though, we will equip RB modules with ACM as needed. If, for example, a table-like structure as in Fig. 1 requires more ACMs, more RB sockets are available. (d) For multiple RB metamodules to handle structural elements in cooperation (future subtask F2, Fig. 1), we envision an in-series coupled, non-actuated, universal joint. The closed kinematic loop of the on-grid floor, a RB metamodule, the handled piece, another RB metamodule, and finally the on-grid table structure imposes strong kinematic constraints. We aim to relax these by adding universal joints between RB metamodules and the to-be-handled piece.

The fastest metamodule off-grid locomotion pattern we found exploited continuously rotating joints and Roombots' shells as wheels. In simulation [44] Roombots modules have shown to be good candidates for studies on the locomotion control of articulated robots with multiple morphologies. Roombots has the potential to alter these morphologies on-the-fly and we are currently studying this topic in hardware.

6. Conclusion

In this work we presented the design of the Roombots (RB) self-reconfiguring modular robotic system. In hardware experiments, we demonstrated locomotion and reconfiguration of single RB modules and RB metamodules (two modules connected in-series) in a 3D structured grid environment. Modules performed on-grid locomotion by "brachiating" along connector ports, overcame concave and convex edges, and climbed up structured walls. RB assemblies also locomoted off-grid, in the non-structured environment, by using rotational or wheel-like locomotion. A mechanism to automatically transfer Roombots modules from off-grid to on-grid was presented, by passive alignment of RB metamodules inside an entrapment mechanism, and a sequence of folding movements to reach an on-grid connector port. Finally, we demonstrated a proof-of-concept of handling light-weight elements. One of Roombots' key components is its strong, latch-based, hermaphrodite, active connection mechanism (ACM). It is capable of compensating for module and connector port misalignments by a scooping movement of its latches. It allows for very flexible integration of Roombots into its environment, through connector ports that can be placed on top of surfaces such as walls, floors, or ceilings, but also light-weight objects. Roombots have a low unit density, compared to other fully lattice-type self-reconfiguring modular robots (Fig. 2). This is advantageous when moving around as a metamodule, or when handling objects and other modules. A Roombots joint can rotate a chain of four RB unit blocks (one metamodule) in any orientation. Roombots' three continuously rotatory DOF allow the module to reconfigure without being limited by joint ranges. Compared to an earlier prototype, we improved RB hardware by a light-weight, stiffer shell design, stronger shell-to-shell fixation through enhanced bearings and joints, and changes increasing the range of the latch scooping movement, and we also tested hybrid ACMs with integrated magnets to increase connection robustness. For the future of the Roombots project we envision our next generation Roombots creating sets of adaptive, shape-changing furniture in our everyday environment. The presented, successful hardware implementation of five sub-scenarios leading towards this goal shows Roombots' potential. The hardware experiments shown and their analysis allowed us to identify necessary improvements, and we have proposed new hardware and design features of a future Roombots generation.

Acknowledgments

We gratefully acknowledge the help of Soha Pouya, Ebru Aidin, Manon Picard, Alexandre Tuleu, Alessandro Crespi, Christophe Chariot, Jocelyn Lotfi, Simon Lepine, Emilie Badri, Philippe Laprade, Thanh-Khai Dinh, Anh The Nguyen, Frédéric Wilhelm, Manuel Stöckli, Yurij Perov, Efthymios Stavridis, Peter Loeppelmann, Jesse van den Kieboom, and Mikaël Mayer for the Roombots project. We gratefully acknowledge the technical support of André Guignard, André Badertscher, Philippe Vosseler, Mitchell Heynick, Jean-Paul Brugger and Manuel Leitos.

This research was supported by the Swiss National Science Foundation through the National Centre of Competence in Research Robotics, the European Community's Seventh Framework Programme FP7/2007–2013—Future Emerging Technologies, Embodied Intelligence, under the grant agreement no. 231688 (Locomorph), and EPFL, Switzerland.

Appendix A. Additional materials

See Tables A.1 and A.2 and Figs. A.19–A.21.

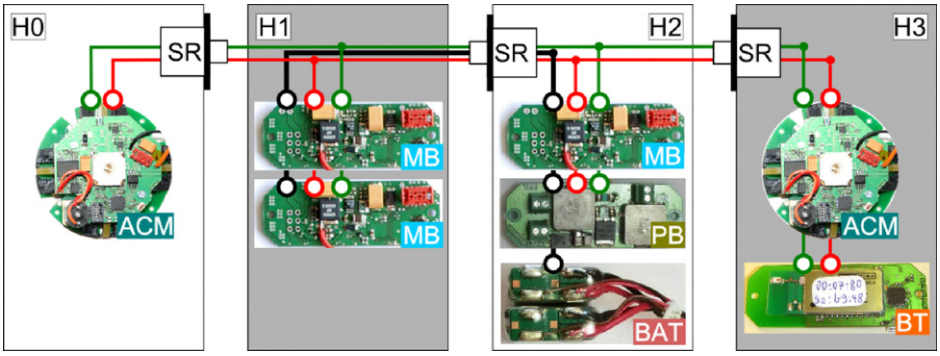

Fig. A.19. Roombots' electronics: active connection mechanism (ACM) control board, motor-driver board (MB), power board (PB), batteries (BAT), Bluetooth communication board (BT), and slip ring (SR). H0, H1, H2, and H3 refer to the half-spheres of Roombots, H0 and H2 are colored white, H1 and H3 are black. The (red) power bus runs a 6 V electrical potential, the black bus a 15 V potential. The green bus is the RS485 communication bus. (For interpretation of the references to colour in this figure legend, the reader is referred to the web version of this article.)

Table A.1
The video is available as support material for this article (see http://dx.doi.org/10.1016/j.robot.2013.08.011).

	Description	Location
1	Five RB subtasks, in order 1–5.	http://www.youtube.com/watch?v=pRlyb9CYG5g

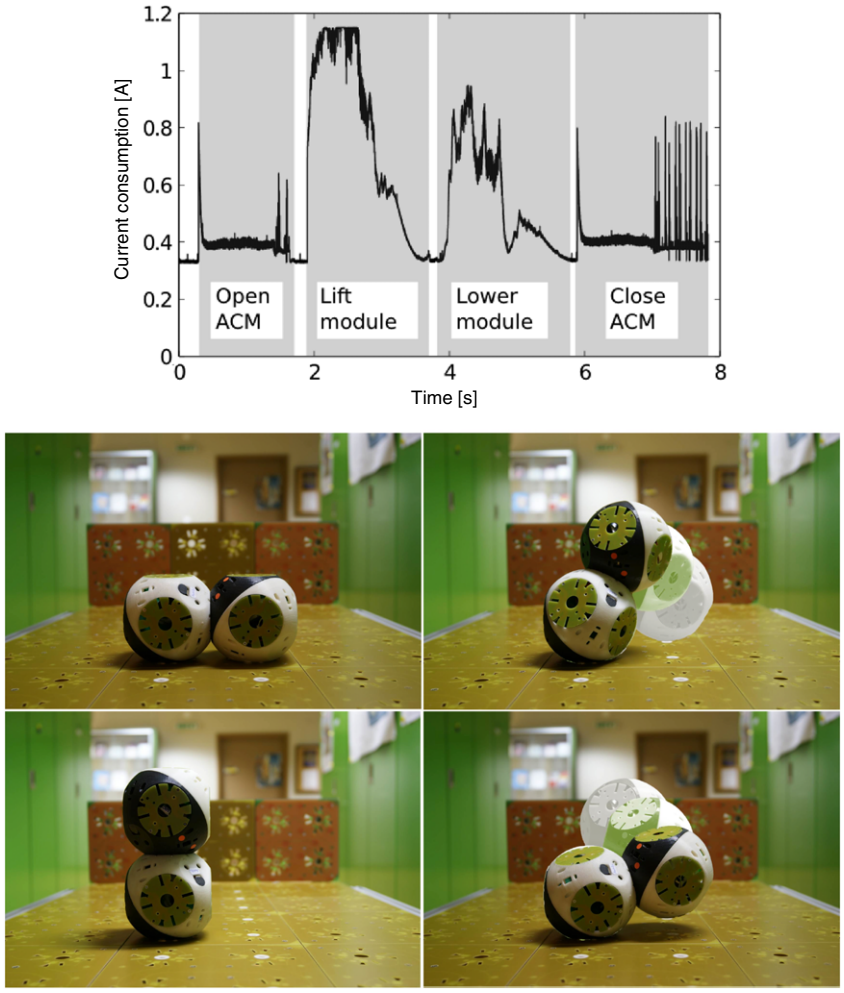

Fig. A.20. Top: instantaneous current consumption of one Roombots module for one possible atomic move, bottom: the corresponding module movements. Initially, the locked active connection mechanics gets released (Open ACM, around 1.1 J). Afterwards, the module lifts itself from the horizontal to the vertical position. Instantaneous currents up to 1.2 A are measured (Lift module). The lift used ≈13 J. The module is rotating back to its horizontal position (Lower module), this used 6.5 J. Lastly, the ACM is re-locked (Close ACM). Locking takes longer than unlocking, as it involves a complex latch–groove interaction (2.6 J). The full sequence took ≈24 J of energy for mechanical actuation. A base power consumption (controller boards, communication) of 5 W (0.35 A at 15 V) is visible from the plot.

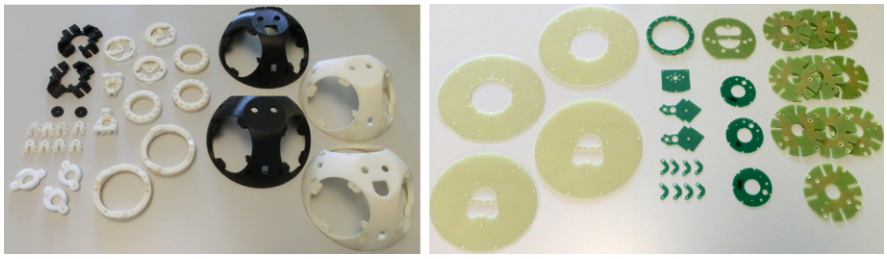

Fig. A.21. Left: Printed elements of one Roombots module. 52% (volume) of RB components are 3D printed from ABS material. Right: glass fiber sheet material used in Roombots.

Table A.2
This table lists 72 modular robots, from 1988 until 2012. Multiple versions of a robot are listed if major changes are documented, e.g. in case of *M-TRAN* [49,33,48,16] and *Molecule* [50,51]. One-purpose snake modular robots are not included in the list: e.g. *Active Cord Mechanism ACM-R4* [52], and *Amphibot II* [53]. The weight and the normalized density of 34 of these robots was extracted, and is plotted in Fig. 2.

	Unit affiliation, Country	Reference	Year
1	**CEBOT** Japan, Science U. of Tokyo	[18,54,55]	1988
2	**RMMS** USA, CMU	[56,57]	1988
3	**PolyPod** USA, Stanford, PARC	[58,59]	1993
4	**Fractum**, **Fracta** Japan, AIST, MEL, MITI	[60]	1994
5	**Metamorphic** USA, Johns Hopkins U.	[61]	1994
6	**Biomorphs** USA, Los Alamos National Laboratory	[62]	1995
7	**MARS** Japan, Nippondenso Co. Ltd, Nagoya U.	[63]	1995
8	**TETROBOT** USA, Rensselaer Polytechnic Institute	[64]	1996
9	**3-D modular units** Japan, AIST, MEL, MITI	[21]	1998
10	**Molecule Robot (v1)** USA, Darthmouth Robotics Lab.	[50]	1998
11	**Self-organizing collective robots**, **Vertical** Japan, Riken, Meiji U.	[65]	1998
12	**CONRO** USA, USC, ISI	[66,67]	1999
13	**ICES Cubes**, **I-Cube** USA, CMU, ICES	[68,69]	1999
14	**Miniaturized Self-reconfigurable System** Japan, AIST	[70]	1999
15	**Reconfigurable Adaptable Micro-robot** USA, Michigan State U.	[71]	1999
16	**Crystalline Robot** USA, Dartmouth College	[72]	2000
17	**M-TRAN** Japan, TiTech, AIST	[49,33]	2000
18	**PolyBot** USA, Xerox PARC	[73]	2000
19	**Proteo** USA, Xerox PARC	[74]	2000
20	**Molecule (v2)** USA, Darthmouth Robotics Lab.	[51]	2002
21	**Pneumatic** Japan, TiTech	[75]	2002
22	**SMC Rover** Japan, TiTech	[76]	2002
23	**Telecubes** USA, Xerox PARC	[19]	2002
24	**M-TRAN II** Japan, AIST, TiTech	[48]	2003
25	**S-BOT (Swarm-bots)** Switzerland, EPFL, IDSIA, Belgium, CENOLI, IRIDIA, Italy, CNR	[17]	2003
26	**Atron** Denmark, USD	[13,77]	2004
27	**Random Parts** USA, MIT	[78,11]	2004
28	**Stochastic** USA, Cornell U.	[10,79]	2004
29	**Catom**, **Programmable matter**, **Claytronics** USA, CMU, Intel Research P.	[80–82]	2005
30	**HYDRA**, **Hydron** Switzerland, UnivZ, USD, U. Of Edinburgh England	[83]	2005
31	**Programmable Parts** USA, U. of Washington	[84]	2005
32	**Slimebot** Japan, Nagoya U., Tohoku U.	[85,86]	2005
33	**Stochastic-3D** USA, Lockheed Martin C., Cornell U.	[79]	2005
34	**AMAS** Japan, TiTech	[87,88]	2006
35	**Deformatron** Denmark, USD	[89]	2006
36	**Superbot** USA, USC	[14]	2006
37	**Y1 Modules** Spain, UAM	[90]	2006
38	**YaMoR** Switzerland, EPFL	[91,15]	2006
39	**Amoeba-I** Japan, Hokkaido U.	[92]	2007
40	**CHOBIE II** Japan, TiTech	[93]	2007
41	**Miche**, **Michelangelo** USA, MIT	[47]	2007
42	**Molecube** USA, Cornell U.	[32,94]	2007
43	**Molecubes open-source** USA, Cornell U.	[95,22]	2007
44	**Shady 3D** USA, MIT	[24,96]	2007
45	**TETwalker**, **ANTS** USA, U. of Kansas	[97]	2007
46	**Tribolon** Switzerland, UnivZ, Denmark, USD	[20]	2007
47	**XBot** USA, Penn	[98,99]	2007
48	**ckBot** USA, Penn, FAMU, FSU	[100]	2008
49	**Em-cube** Republic of Korea, DCS lab	[101]	2008
50	**GZ-I Modules** Germany, U. of Hamburg, Spain, UAM, China, ZUT	[102]	2008
51	**M-TRAN III** Japan, AIST, U. of Tsukuba, TiTech	[16]	2008
52	**MinDART** USA, U. of Minnesota	[103]	2008
53	**Morpho** USA, Harvard, MIT	[104]	2008
54	**Odin** Denmark, USD	[8]	2008
55	**Symbrion** Germany, U. of Stuttgart	[105]	2008
56	**Raupi** Germany, Ilmenau TU	[106]	2009
57	**Roombots** Switzerland, EPFL	[107,41]	2009
58	**Ubot** China, HIT	[108]	2009
59	**Actuated Responsive Truss** Canada, U. of Toronto	[109]	2010
60	**Factory Floor** USA, Penn	[110]	2010
61	**iMobot** USA, U. of California	[111]	2010
62	**Kilobot** USA, Harvard U.	[112]	2010
63	**Modular-Expanding Robots** USA, Franklin W. Olin CoE, Harvard U.	[113]	2010
64	**Pebbles** USA, MIT	[114]	2010
65	**Sambot** China, Beihang University	[115]	2010
66	**Thor modular robot** Denmark, USD	[116]	2010

Table A.2 (*continued*)

	Unit affiliation, Country	Reference	Year
67	**Vacuubes** USA, Cornell U., Denmark, USD	[117]	2010
68	**HitMSR II** China, HIT	[118]	2011
70	**ModRED** USA, UNL, UNO	[119]	2012
71	**Smart Blocks** France, U. de Franche-Compte, Germany, Ilmenau U. Of Technology	[120]	2012
72	**SMORES** Australia, U. of South Wales, USA, Penn	[121]	2012

References

[1] Y. Terada, S. Murata, Automatic assembly system for a large-scale modular structure: hardware design of module and assembler robot, in: Proceedings of IROS04, 2004, pp. 2349–2355.

[2] S.-K. Yun, D.A. Hjelle, E. Schweikardt, H. Lipson, D. Rus, Planning the reconfiguration of grounded truss structures with truss climbing robots that carry truss elements, in: IEEE International Conference on Robotics and Automation, 2009, ICRA'09, IEEE, 2009, pp. 1327–1333.

[3] A.J. Ijspeert, Central pattern generators for locomotion control in animals and robots: a review, Neural Networks 21 (4) (2008) 642–653.

[4] A. Spröwitz, Roombots: design and implementation of a modular robot for reconfiguration and locomotion, Ph.D. Thesis, Lausanne, 2010. http://dx.doi.org/10.5075/epfl-thesis-4803.

[5] S. Bonardi, R. Moeckel, A. Spröwitz, M. Vespignani, A. Ijspeert, Locomotion through reconfiguration based on motor primitives for roombots self-reconfigurable modular robots, in: 7th German Conference on Robotics—Robotik 2012, 2012.

[6] T. Fukuda, Y. Kawauchi, Cellular robotic system (CE-BOT) as one of the realization of self-organizing intelligent universal manipulators, in: Proc. of IEEE ICRA, 1990, 1990.

[7] M. Yim, W. Shen, B. Salemi, D. Rus, M. Moll, H. Lipson, E. Klavins, G. Chirikjian, Modular self-reconfigurable robot systems: challenges and opportunities for the future, IEEE Robotics and Automation Magazine 14 (1) (2007) 43–52.

[8] A. Lyder, R. Garcia, K. Stoy, Mechanical design of odin, an extendable heterogeneous deformable modular robot, in: IEEE/RSJ International Conference on Intelligent Robots and Systems, 2008, IROS 2008, 2008, pp. 883–888.

[9] V. Zykov, H. Lipson, Fluidic stochastic modular robotics: revisiting the system design, in: Proceedings of Robotics Science and Systems Workshop on Self-Reconfigurable Modular Robots, Philadelphia PA, 2006.

[10] P. White, K. Kopanski, H. Lipson, Stochastic self-reconfigurable cellular robotics, in: 2004 IEEE International Conference on Robotics and Automation, 2004. Proceedings, ICRA'04, vol. 3, 2004, pp. 2888–2893.

[11] S. Griffith, D. Goldwater, J.M. Jacobson, Robotics: self-replication from random parts, Nature 437 (7059) (2005) 636.

[12] P.W.K. Rothemund, Folding DNA to create nanoscale shapes and patterns, Nature 440 (7082) (2006) 297–302. http://dx.doi.org/10.1038/nature04586.

[13] M. Jørgensen, E. Østergaard, H. Lund, Modular ATRON: modules for a self-reconfigurable robot, in: IEEE/RSJ Int. Conf. on Robots and Systems, Sendai, Japan, 2004, pp. 2068–2073.

[14] W. Shen, M. Krivokon, H. Chiu, J. Everist, M. Rubenstein, J. Venkatesh, Multimode locomotion via SuperBot reconfigurable robots, Autonomous Robots 20 (2) (2006) 165–177.

[15] A. Spröwitz, R. Moeckel, J. Maye, A. Ijspeert, Learning to move in modular robots using central pattern generators and online optimization, International Journal of Robotics Research 27 (3–4) (2008) 423–443.

[16] H. Kurokawa, K. Tomita, A. Kamimura, S. Kokaji, T. Hasuo, S. Murata, Distributed self-reconfiguration of M-TRAN III modular robotic system, The International Journal of Robotics Research 27 (3–4) (2008) 373–386.

[17] F. Mondada, G.C. Pettinaro, A. Guignard, I.W. Kwee, D. Floreano, J. Deneubourg, S. Nolfi, L.M. Gambardella, M. Dorigo, Swarm-Bot: a new distributed robotic concept, Autonomous Robots 17 (2) (2004) 193–221.

[18] T. Fukuda, S. Nakagawa, Approach to the dynamically reconfigurable robot systems, Journal of Intelligent Robtics Systems 1 (1988) 55–72.

[19] J. Suh, S. Homans, M. Yim, Telecubes: mechanical design of a module for self-reconfigurable robotics, in: IEEE International Conference on Robotics and Automation, 2002. Proceedings, ICRA'02, vol. 4, 2002, pp. 4095–4101.

[20] S. Miyashita, M. Hadorn, P. Hotz, Water floating self-assembling agents, in: Agent and Multi-Agent Systems: Technologies and Applications, 2007, pp. 665–674.

[21] S. Murata, H. Kurokawa, E. Yoshida, S. Tomita, K. Kokaji, A 3-D self-reconfigurable structure, in: 1998 IEEE International Conference on Robotics and Automation, 1998. Proceedings, vol. 1, 1998, pp. 432–439.

[22] V. Zykov, A. Chan, H. Lipson, Molecubes: an open-source modular robotics kit, in: Proceedings of IROS2007, Workshop on Self-Reconfigurable Modular Robots and System Applications, San Diego, CA, USA, 2007.

[23] J. Bongard, V. Zykov, H. Lipson, Resilient machines through continuous self-modeling, Science 314 (5802) (2006) 1118–1121.

[24] Y. Yoon, D. Rus, Shady3D: a robot that climbs 3D trusses, in: 2007 IEEE International Conference on Robotics and Automation, 2007, pp. 4071–4076.

[25] D. Rus, M. Vona, Crystalline robots: self-reconfiguration with compressible unit modules, Autonomous Robots 10 (1) (2001) 107–124.

[26] J. Neubert, A. Cantwell, S. Constantin, M. Kalontarov, D. Erickson, H. Lipson, A robotic module for stochastic fluidic assembly of 3D self-reconfiguring structures, in: 2010 IEEE International Conference on Robotics and Automation, ICRA, 2010, pp. 2479–2484.

[27] S. Revzen, M. Bhoite, A. Macasieb, M. Yim, Structure synthesis on-the-fly in a modular robot, in: 2011 IEEE/RSJ International Conference on Intelligent Robots and Systems, IROS, 2011, pp. 4797–4802.

[28] L. Wang, F. Iida, Physical connection and disconnection control based on hot melt adhesives, IEEE/ASME Transactions on Mechatronics 18 (4) (2012) 1397–1409.

[29] M. Vona, C. Detweiler, D. Rus, Shady: robust truss climbing with mechanical compliances, in: Experimental Robotics, vol. 38, 2008, pp. 431–440.

[30] D. Rus, Z. Butler, K. Kotay, M. Vona, Self-reconfiguring robots, Communications of the ACM Archive 45 (2002) 39–45.

[31] S. Miyashita, F. Casanova, M. Lungarella, R. Pfeifer, Peltier-based freeze-thaw connector for waterborne self-assembly systems, in: IEEE/RSJ International Conference on Intelligent Robots and Systems, 2008, IROS 2008, 2008, pp. 1325–1330.

[32] V. Zykov, E. Mytilinaios, B. Adams, H. Lipson, Self-reproducing machines, Nature 435 (7038) (2005) 163–164.

[33] S. Murata, E. Yoshida, A. Kamimura, H. Kurokawa, K. Tomita, S. Kokaji, M-TRAN: self-reconfigurable modular robotic system, IEEE/ASME Transactions on Mechatronics 7 (4) (2002) 431–441.

[34] W.-M. Shen, M. Krivokon, H. Chiu, J. Everist, M. Rubenstein, J. Venkatesh, Multimode locomotion via SuperBot reconfigurable robots, Autonomous Robots 20 (2) (2006) 165–177.

[35] E. Badri, Elasticity compensation using explicit learning, Master Project, Ecole Polytechnique Federale de Lausanne, Switzerland, 2011.

[36] Linear Technology Inc. http://www.linear.com/.

[37] Analog Devices Inc. http://www.analog.com/.

[38] Microchip Inc. http://www.microchip.com/.

[39] Bluegiga Technologies Inc. http://www.bluegiga.com/.

[40] Allegro Microsystems Inc. http://www.allegromicro.com/.

[41] A. Spröwitz, S. Pouya, S. Bonardi, J. van den Kieboom, R. Moeckel, A. Billard, P. Dillenbourg, A. Ijspeert, Roombots: reconfigurable robots for adaptive furniture, IEEE Computational Intelligence Magazine 5 (3) (2010) 20–32. http://dx.doi.org/10.1109/MCI.2010.937320. Special issue on "Evolutionary and developmental approaches to robotics".

[42] A. Spröwitz, P. Laprade, S. Bonardi, M. Mayer, R. Möckel, P.-A. Mudry, A.J. Ijspeert, Roombots-towards decentralized reconfiguration with self-reconfiguring modular robotic metamodules, in: Proceedings of IROS 2010, 2010.

[43] K. Stoy, Using cellular automata and gradients to control self-reconfiguration, Robotics and Autonomous Systems 54 (2) (2006) 135–141.

[44] S. Pouya, J. van den Kieboom, A. Spröwitz, A. Ijspeert, Automatic gait generation in modular robots: to oscillate or to rotate? That is the question, in: Proceedings of IROS 2010, 2010.

[45] A.T. Nguyen, Online optimization for the locomotion of roombots, Semester Project, Ecole Polytechnique Federale de Lausanne, Switzerland, 2012.

[46] T.-K. Dinh, Grid alignment and extendable grid for roombots, Semester Project, Ecole Polytechnique Federale de Lausanne, Switzerland, 2010.

[47] K. Gilpin, K. Kotay, D. Rus, I. Vasilescu, Miche: modular shape formation by self-disassembly, The International Journal of Robotics Research 27 (3–4) (2008) 345–372.

[48] H. Kurokawa, A. Kamimura, E. Yoshida, K. Tomita, S. Kokaji, S. Murata, M-TRAN II: metamorphosis from a four-legged walker to a caterpillar, in: Proceedings. 2003 IEEE/RSJ International Conference on Intelligent Robots and Systems, 2003, IROS 2003, vol. 3, 2003, pp. 2454–2459.

[49] H. Kurokawa, K. Tomita, E. Yoshida, S. Murata, S. Kokaji, Motion simulation of a modular robotic system, in: Proc. of 26th Annual Conference of the IEEE Industrial Electronics Society, 2000, IECON 2000, 2000, pp. 2473–2478.

[50] K. Kotay, D. Rus, Locomotion versatility through self-reconfiguration, Robotics and Autonomous Systems 26 (1998) 217–232.

[51] D. Rus, Z. Butler, K. Kotay, M. Vona, Self-reconfiguring robots, Communications of the ACM 45 (3) (2002) 39–45.

[52] H. Yamada, S. Hirose, Development of practical 3-dimensional active cord mechanism ACM-R4, Journal of Robotics and Mechatronics 18 (3) (2006) 305–311.

[53] A. Crespi, A.J. Ijspeert, AmphiBot II: an amphibious snake robot that crawls and swims using a central pattern generator, in: Proceedings of the 9th International Conference on Climbing and Walking Robots, CLAWAR 2006, 2006, pp. 19–27.

[54] T. Fukuda, S. Nakagawa, Y. Kawauchi, M. Buss, Self organizing robots based on cell structures—CEBOT, in: IEEE/RSJ Int. Conf. on Intelligent Robots and Systems, 1988, pp. 145–150.

[55] T. Fukuda, T. Ueyama, Y. Kawauchi, F. Arai, Concept of cellular robotic system (CEBOT) and basic strategies for its realization, Computers & Electrical Engineering 18 (1) (1992) 11–39.
[56] D. Schmitz, P. Kho, T. Kanade, The CMU reconfigurable modular manipulator system, Technical Report CMU-RI-TR-88-07, The Robotics Institute, Carnegie Mellon University, Pittsburgh, PA, 1988.
[57] C. Paredis, H. Brown, P. Khosla, A rapidly deployable manipulator system, Robotics and Autonomous Systems 21 (3) (1997) 289–304.
[58] M. Yim, A reconfigurable modular robot with many modes of locomotion, in: Proc. of Intl. Conf. on Advanced Mechatronics, 1993, pp. 283–288.
[59] M. Yim, Locomotion with a unit-modular reconfigurable robot, Ph.D., Stanford University, 1995.
[60] S. Murata, H. Kurokawa, S. Kokaji, Self-assembling machine, in: 1994 IEEE International Conference on Robotics and Automation, 1994. Proceedings, vol. 1, 1994, pp. 441–448.
[61] G. Chirikjian, Kinematics of a metamorphic robotic system, in: 1994 IEEE International Conference on Robotics and Automation, 1994. Proceedings, vol. 1, 1994, pp. 449–455.
[62] B. Hasslacher, M. Tilden, Living machines, Robotics and Autonomous Systems 15 (1995) 143–169.
[63] N. Mitsumoto, T. Fukuda, K. Shimojima, A. Ogawa, Micro autonomous robotic system and biologically inspired immune swarm strategy as a multi agent robotic system, in: 1995 IEEE International Conference on Robotics and Automation, 1995. Proceedings, vol. 2, 1995, pp. 2187–2192.
[64] G. Hamlin, A. Sanderson, TETROBOT modular robotics: prototype and experiments, in: Proceedings of the 1996 IEEE/RSJ International Conference on Intelligent Robots and Systems'96, IROS 96, vol. 2, 1996, pp. 390–395.
[65] K. Hosokawa, T. Tsujimori, T. Fujii, H. Kaetsu, H. Asama, Y. Kuroda, I. Endo, Self-organizing collective robots with morphogenesis in a vertical plane, in: 1998 IEEE International Conference on Robotics and Automation, 1998. Proceedings, vol. 4, 1998, pp. 2858–2863.
[66] P.M. Will, A. Castano, W. Shen, Robot modularity for self-reconfiguration, in: G.T. McKee, P.S. Schenker (Eds.), Sensor Fusion and Decentralized Control in Robotic Systems II, vol. 3839, SPIE, Boston, MA, USA, 1999, pp. 236–245.
[67] A. Castano, W. Shen, P. Will, Conro: towards deployable robots with inter-robots metamorphic capabilities, Autonomous Robots 8 (3) (2000) 309–324.
[68] C. Ünsal, H. Kiliccote, P. Khosla, I(CES)-cubes: a modular self-reconfigurable bipartite robotic system, in: G.T. McKee, P.S. Schenker (Eds.), Sensor Fusion and Decentralized Control in Robotic Systems II, vol. 3839, SPIE, Boston, MA, USA, 1999, pp. 258–269.
[69] C. Ünsal, H. Kiliççöte, P. Khosla, A modular self-reconfigurable bipartite robotic system: implementation and motion planning, Autonomous Robots 10 (1) (2001) 23–40.
[70] E. Yoshida, S. Kokaji, S. Murata, H. Kurokawa, K. Tomita, Miniaturized self-reconfigurable system using shape memory alloy, in: 1999 IEEE/RSJ International Conference on Intelligent Robots and Systems, 1999, IROS'99. Proceedings, vol. 3, 1999, pp. 1579–1585.
[71] R.L. Tummala, R. Mukherjee, D. Aslam, N. Xi, S. Mahadevan, J. Weng, Reconfigurable adaptable micro-robot, in: 1999 IEEE International Conference on Systems, Man, and Cybernetics, 1999, IEEE SMC'99 Conference Proceedings, vol. 6, 1999, pp. 687–691.
[72] D. Rus, M. Vona, A physical implementation of the self-reconfiguring crystalline robot, in: PROC. IEEE Int. Conf. Rob. Autom., vol. 2, 2000, pp. 1726—1733.
[73] M. Yim, D. Duff, K. Roufas, PolyBot: a modular reconfigurable robot, in: Proc. IEEE Int. Conf. Rob. Autom., vol. 1, 2000, pp. 514–520.
[74] H. Bojinov, A. Casal, T. Hogg, Emergent structures in modular self-reconfigurable robots, in: IEEE International Conference on Robotics and Automation, 2000. Proceedings, ICRA'00, vol. 2, 2000, pp. 1734–1741.
[75] N. Inou, H. Kobayashi, M. Koseki, Development of pneumatic cellular robots forming a mechanical structure, in: 7th International Conference on Control, Automation, Robotics and Vision, 2002, ICARCV 2002, vol. 1, 2002, pp. 63–68.
[76] A. Kawakami, A. Torii, K. Motomura, S. Hirose, SMC rover: planetary rover with transformable wheels, in: SICE 2002. Proceedings of the 41st SICE Annual Conference, vol. 1, 2002, pp. 157–162.
[77] D.J. Christensen, M. Bordignon, U.P. Schultz, D. Shaikh, K. Stoy, Morphology independent learning in modular robots, in: Distributed Autonomous Robotic Systems, vol. 8, 2009, pp. 379–391.
[78] S. Griffith, Growing machines, Thesis, Massachusetts Institute of Technology, USA, MIT, School of Architecture and Planning, Program in Media Arts and Sciences, 2004.
[79] P. White, V. Zykov, J. Bongard, H. Lipson, Three dimensional stochastic reconfiguration of modular robots, in: Proceedings of Robotics Science and Systems, 2005, pp. 161–168.
[80] S. Goldstein, J. Campbell, T. Mowry, Programmable matter, Computer 38 (6) (2005) 99–101.
[81] J. Campbell, P. Pillai, Collective actuation, The International Journal of Robotics Research 27 (3–4) (2008) 299–314.
[82] B. Aksak, J. Campbell, J. Hoburg, T. Mowry, P. Pillai, S. Goldstein, B. Kirby, A modular robotic system using magnetic force effectors, in: IEEE/RSJ International Conference on Intelligent Robots and Systems, 2007, IROS 2007, 2007, pp. 2787–2793.
[83] E. Ostergaard, D. Christensen, P. Eggenberger, T. Taylor, P. Ottery, H. Lund, HYDRA: from cellular biology to shape-changing artefacts, in: Artificial Neural Networks: Biological Inspirations ICANN 2005, 2005, pp. 275–281.
[84] J. Bishop, S. Burden, E. Klavins, R. Kreisberg, W. Malone, N. Napp, T. Nguyen, Programmable parts: a demonstration of the grammatical approach to self-organization, in: 2005 IEEE/RSJ International Conference on Intelligent Robots and Systems, 2005, IROS 2005, 2005, pp. 3684–3691.
[85] M. Shimizu, A. Ishiguro, T. Kawakatsu, Slimebot: a modular robot that exploits emergent phenomena, in: Proceedings of the 2005 IEEE International Conference on Robotics and Automation, 2005, ICRA 2005, 2005, pp. 2982–2987.
[86] M. Shimizu, T. Kato, M. Lungarella, A. Ishiguro, Adaptive reconfiguration of a modular robot through heterogeneous inter-module connections, in: Proc. of the 2008 IEEE Int. Conf. on Robotics and Automation, 2008, pp. 3527–3532.
[87] Y. Terada, S. Murata, Modular structure assembly using blackboard path planning system, in: Proc of ISARC2006, 2006, pp. 852–857.
[88] Y. Terada, S. Murata, Automatic modular assembly system and its distributed control, The International Journal of Robotics Research 27 (3–4) (2008) 445–462.
[89] K. Stoy, The deformatron robot: a biologically inspired homogeneous modular robot, in: Proceedings 2006 IEEE International Conference on Robotics and Automation, 2006, ICRA 2006, IEEE, 2006, pp. 2527–2531.
[90] J. Gonzalez-Gomez, E. Boemo, Motion of minimal configurations of a modular robot: sinusoidal, lateral rolling and lateral shift, in: Climbing and Walking Robots, 2006, pp. 667–674.
[91] R. Möckel, C. Jaquier, K. Drapel, E. Dittrich, A. Upegi, A.J. Ijspeert, Exploring adaptive locomotion with YaMoR, a novel autonomous modular robot with bluetooth interface, Industrial Robot: An International Journal 33 (4) (2006) 285–290.
[92] J. Liu, Y. Wang, B. Li, S. Ma, D. Tan, Center-configuration selection technique for the reconfigurable modular robot, Science in China Series F: Information Sciences 50 (5) (2007) 697–710.
[93] Y. Suzuki, N. Inou, H. Kimura, M. Koseki, Reconfigurable group robots adaptively transforming a mechanical structure-numerical expression of criteria for structural transformation and automatic motion planning method, in: IEEE/RSJ International Conference on Intelligent Robots and Systems, 2007, IROS 2007, IEEE, 2007, pp. 2361–2367.
[94] V. Zykov, E. Mytilinaios, M. Desnoyer, H. Lipson, Evolved and designed self-reproducing modular robotics, IEEE Transactions on Robotics 23 (2) (2007) 308–319.
[95] V. Zykov, P. Williams, N. Lassabe, H. Lipson, Molecubes extended: diversifying capabilities of open-source modular robotics, in: International Conference on Intelligent RObots and Systems, Self-Reconfigurable Robots Workshop, 2008.
[96] S. Yun, D. Rus, Self assembly of modular manipulators with active and passive modules, in: IEEE International Conference on Robotics and Automation, 2008, ICRA 2008, 2008, pp. 1477–1482.
[97] B.L. Carmichael, C.M. Gifford, Modeling and simulation of the seismic TETwalker concept, Technical Report CReSIS TR 134, University of Kansas, 2007.
[98] P. White, M. Yim, Scalable modular self-reconfigurable robots using external actuation, in: Proceedings of IEEE/RSJ International Conference on Intelligent Robots and Systems, 2007, IROS 2007, 2007, pp. 2773–2778.
[99] P. White, M. Yim, Reliable external actuation for full reachability in robotic modular self-reconfiguration, The International Journal of Robotics Research 29 (5) (2010) 1–15.
[100] J. Sastra, W. Heredia, J. Clark, M. Yim, A biologically-inspired dynamic legged locomotion with a modular reconfigurable robot, in: ASME 2008 Dynamic Systems and Control Conference, Parts A and B, 2008, pp. 1467–1474.
[101] B. An, Em-cube: cube-shaped, self-reconfigurable robots sliding on structure surfaces, in: Proc. of IEEE International Conference on Robotics and Automation, 2008, ICRA 2008, 2008, pp. 3149–3155.
[102] H. Zhang, J. Gonzalez-Gomez, Z. Me, S. Cheng, J. Zhang, Development of a low-cost flexible modular robot GZ-I, in: IEEE/ASME International Conference on Advanced Intelligent Mechatronics, 2008, AIM 2008, 2008, pp. 223–228.
[103] P. Rybski, A. Larson, H. Veeraraghavan, M. Anderson, M. Gini, Performance evaluation of a multi-robot search & retrieval system: experiences with MinDART, Journal of Intelligent and Robotic Systems 52 (3) (2008) 363–387.
[104] C. Yu, K. Haller, D. Ingber, R. Nagpal, Morpho: a self-deformable modular robot inspired by cellular structure, in: Proc. of IEEE/RSJ International Conference on Intelligent Robots and Systems, 2008, IROS 2008, 2008, pp. 3571–3578.
[105] S. Kernbach, E. Meister, F. Schlachter, K. Jebens, M. Szymanski, J. Liedke, D. Laneri, L. Winkler, T. Schmickl, R. Thenius, P. Corradi, L. Ricotti, Symbiotic robot organisms: REPLICATOR and SYMBRION projects, in: Proceedings of the 8th Workshop on Performance Metrics for Intelligent Systems, ACM, Gaithersburg, Maryland, 2008, pp. 62–69.
[106] J. Mämpel, K. Gerlach, C. Schilling, H. Witte, A modular robot climbing on pipe-like structures, in: Proceedings of the 4th International Conference on Autonomous Robots and Agents, Wellington, New Zealand, 2009, pp. 87–91.
[107] A. Spröwitz, A. Billard, P. Dillenbourg, A.J. Ijspeert, Roombots-mechanical design of self-reconfiguring modular robots for adaptive furniture, in: Proceedings of 2009 IEEE International Conference on Robotics and Automation, 2009, pp. 4259–4264.
[108] S. Tang, Y. Zhu, J. Zhao, X. Cui, The ubot modules for self-reconfigurable robot, in: ASME/IFToMM International Conference on Reconfigurable Mechanisms and Robots, 2009, ReMAR 2009, IEEE, 2009, pp. 529–535.
[109] R. Merali, D. Long, Actuated responsive truss, in: Proc. of ICRA 2010 Workshop Modular Robots: State of the Art, 2010, pp. 36–40.

[110] K. Galloway, R. Jois, M. Yim, Factory floor: a robotically reconfigurable construction platform, in: 2010 IEEE International Conference on Robotics and Automation, ICRA, IEEE, 2010, pp. 2467–2472.
[111] D. Ko, H.H. Chen, G.G. Ryland, Reconfigurable software for reconfigurable modular robots, in: Proc. of ICRA 2010 Workshop Modular Robots: State of the Art, 2010, pp. 100–105.
[112] M. Rubenstein, R. Nagpal, Kilobot: a robotic module for demonstrating behaviors in a large scale (210 units) collective, in: Proc. of ICRA 2010 Workshop Modular Robots: State of the Art, 2010, pp. 47–51.
[113] R. Belisle, C. Yu, R. Nagpal, Mechanical design and locomotion of modular-expanding robots, in: Proc. of ICRA 2010 Workshop Modular Robots: State of the Art, 2010, pp. 17–23.
[114] K. Gilpin, D. Rus, Self-disassembling robots pebbles: new results and ideas for self-assembly of 3D structures, in: Proc. of ICRA 2010 Workshop Modular Robots: State of the Art, 2010, pp. 94–99.
[115] H. Wei, Y. Chen, J. Tan, T. Wang, Sambot: a self-assembly modular robot system, IEEE/ASME Transactions on Mechatronics 16 (4) (2011) 745–757.
[116] A. Lyder, R.F.M. Garcia, K. Stoy, Genderless connection mechanism for modular robots introducing torque transmission between modules, in: Proc. of ICRA 2010 Workshop Modular Robots: State of the Art, 2010, pp. 77–81.
[117] R. Garcia, J. Hiller, H. Lipson, A vacuum-based bonding mechanism for modular robotics, in: Proc. of ICRA 2010 Workshop Modular Robots: State of the Art, 2010, pp. 57–62.
[118] Y. Zhu, X. Wang, X. Cui, J. Yin, J. Zhao, Research on locomotive evolution based on worm-shaped configuration of self-reconfigurable robot hitmsr II, Electrical Power Systems and Computers (2011) 245–252.
[119] S. Hossain, C. Nelson, P. Dasgupta, Hardware design and testing of modred: a modular self-reconfigurable robot system, in: Advances in Reconfigurable Mechanisms and Robots I, 2012, pp. 515–523.
[120] S. Mobes, G. Laurent, C. Clévy, L. Fort-Piat, B. Piranda, J. Bourgeois, et al., Toward a 2D modular and self-reconfigurable robot for conveying microparts, in: 2012 Second Workshop on Design, Control and Software Implementation for Distributed MEMS, dMEMS, IEEE, 2012, pp. 7–13.
[121] J. Davey, N. Kwok, M. Yim, Emulating self-reconfigurable robots-design of the smores system, in: 2012 IEEE/RSJ International Conference on Intelligent Robots and Systems, IROS, IEEE, 2012, pp. 4464–4469.

Alexander Spröwitz is a post-doctoral researcher. He worked until 2013 at the Biorobotics Laboratory, EPFL, Switzerland. He has a "Vordiplom" (B.Sc.) in Mechanical Engineering, and a "Diplom" (M.Sc.) in Biomechatronics from the University of Ilmenau, Germany, and a Ph.D. in Manufacturing Systems and Robotics from EPFL, Switzerland. His research includes design and control of self-reconfiguring modular robots and bipedal and quadrupedal legged robots, and biomechanics of legged robotic and animal locomotion, such as in running birds.

Rico Moeckel is a post-doctoral researcher. He received a Ph.D. degree from the Swiss Federal Institute of Technology in Zurich, Switzerland, and a diploma (equivalent to M.Sc.) in Electrical Engineering from the University of Rostock, Germany. His research interests are in the fields of legged and modular robotics, computational neuroscience, locomotion control and VLSI vision sensors.

Massimo Vespignani is a Ph.D. student in the Biorobotics Laboratory (BioRob) at EPFL. He received his M.S. degree in Biomedical Engineering from the Campus Bio-Medico University (Rome, Italy) in 2009. His research interests include reconfiguring modular robotic systems, mechanical design, bio-inspired robotics, legged locomotion and soft robotics.

Stephane Bonardi received a M.Sc. (engineering diploma) in Applied Mathematics and Modeling from the Institut des Sciences et Techniques de l'Ingenieur de Lyon (ISTIL-EPU) in 2009. He joined the Biorobotics Laboratory as a Ph.D. student in February 2010. He is working on the Roombots project, mainly on the aspects of self-reconfiguration and end-user interface.

Auke Jan Ijspeert is an associate professor at the EPFL (Ecole Polytechnique Federale de Lausanne, Switzerland), and head of the Biorobotics Laboratory. He has a "diplome d'ingenieur" in physics from the EPFL, and a Ph.D. in artificial intelligence from the University of Edinburgh. His research interests are at the intersection between robotics, computational neuroscience, nonlinear dynamical systems, and applied machine learning. He is interested in using numerical simulations and robots to get a better understanding of the sensorimotor coordination in animals, and in using inspiration from biology to design novel types of robots and adaptive controllers (see for instance Ijspeert et al. Science, vol. 315: 5817, pp. 1416–1420, 2007). For more information see: http://biorob.epfl.ch.